AD-A077 576 RAYTHEON CO WALTHAM MASS MICROWAVE AND POWER TUBE DIV F/G 9/1
DUAL BEAM DUAL MODE TWT.(U)
NOV 78
UNCLASSIFIED PT-5289 N00014-78-C-0791
NL

| OF |
AD
A077576

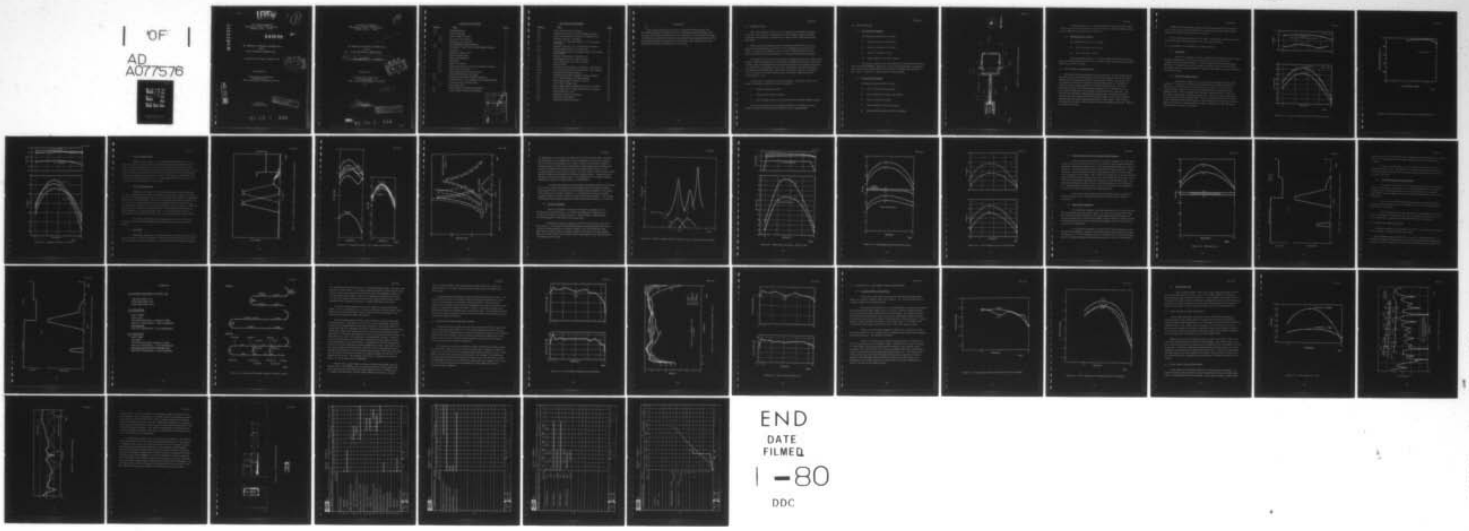

END
DATE
FILMED
| -80
DDC

RAYTHEON COMPANY
Microwave and Power Tube Division
Waltham, Mass. 02154

BI- MONTHLY PROGRESS REPORT NO. 1
FOR A
DUAL BEAM DUAL MODE TWT

15 August 1978 through 15 October 1978

Prepared For

Naval Research Laboratory
Washington D.C.
Under Contract No. N00014-78-C-0791

PT-5289
8 November 1978

(1)

RAYTHEON COMPANY
Microwave and Power Tube Division
Waltham, Mass. 02154

#2 - AD B040517L

BI- MONTHLY PROGRESS REPORT NO. 1

FOR A

(6) DUAL BEAM DUAL MODE TWT

(9) Bi-Monthly Progress Rept. No. 1,
15 August ~~1978~~ through 15 October ~~1978~~

Prepared For

Naval Research Laboratory
Washington D.C.
Under Contract No. (15) N00014-78-C-0791

(12) 47

(14) PT-5289
(11) 8 November ~~1978~~

[redacted]

298 310

JOB

TABLE OF CONTENTS

Section	Title	Page
1.0	INTRODUCTION	1
2.0	TEST VEHICLES	2
2.1	Heat Transfer Vehicles	2
2.2	Insertion Loss Vehicles	2
2.3	Attenuation Test Vehicles	4
3.0	HEAT SHRINK IMPROVEMENT	4
4.0	CW STAGE - NEW DESIGN FOR HIGHER POWER	5
4.1	Simulation	5
4.2	Scaling for Higher Power	5
4.3	Main Attenuator Shift	9
4.4	Buffer Tail Elongation	9
4.5	Input BWO	9
4.6	Design Version K1	13
4.7	Design Version K2 - Reduced Input Helix Diameter	18
4.8	Input Buffer Attenuator	18
4.9	Input Oscillation Threshold Analysis	21
5.0	COMPUTER MODEL OF CHAIN	21
6.0	SEPARATE POWER SUPPLIES TESTING	26
7.0	PULSE STAGE - NEW DESIGN FOR HIGHER POWER	30
7.1	Computer Model of Pulse Stage	30
7.2	Pulse Stage CAD	33
8.0	COAX-TO-WAVEGUIDE TRANSITION	33
9.0	DUAL STAGE COLLECTOR DESIGN	33

LIST OF ILLUSTRATIONS

Section	Title	Page
2-1	Heat Transfer Vehicle Layout.	3
4-1	Computer Simulation of S/N 17 Power and Gain.	6
4-2	Beam Transmission vs Current CW Stage S/N 17.	7
4-3	Computer Scaling - CW Stage.	8
4-4	Loss Pattern - Baseline and B, C, D, E Versions CW Stage.	10
4-5	Computer Results - CW - Buffer Tail Variation.	11
4-6	BWO Computer Data for Lossless CW	12
4-7	BWO Computer Data for Lossless Lines - K1 Version vs Baseline.	14
4-8	Expected Performance - SIM K1, K2.	15
4-9	Small Signal Gain K1 and K2 Versions.	16
4-10	Gain Comparison, K1 vs K2 Versions.	17
4-11	Saturated Gain	19
4-12	Circuit Loss and Velocity vs Distance - K5 Version.	20
4-13	Circuit Loss and Velocity vs Distance - K16 Version.	22
4-14	Oscillation Threshold Analysis	23
5-1	Oscillation Threshold Computer Program Layout	24
6-1	S/N 17 Single Voltage Test Pulse Stage.	27
6-2	Pulse Stage Voltage Variation - S/N 17.	28
6-3	S/N 17 Dual Voltage Test.	29
7-1	Power Output Pdbm at Watts Drive S/N 17 vs Model.	31
7-2	Power Output at P-10 Watt Drive S/N 17 vs Model.	32
7-3	Pulse Mode Gain - L61.	34
8-1	Waveguide Transistion Results	35
8-2	50 Ω Coax to Waveguide.	36
9-1	Preliminary Package Layout.	38

ABSTRACT

This report describes the activities during the first two months of a development program designed to bring an existing high-band dual mode TWT up to the recent JSC specification for dual mode tubes. Test vehicles for design verification testing have been designed and ordered, tube design has been carried out, tooling improvements have been implemented, and design work on a new waveguide transition and collectors is described.

1.0 INTRODUCTION

The work described in this report is being done for the Office of Naval Research. The program is an outgrowth of work begun in 1974 for the ONR directed towards building a 10 dB pulse-up, liquid cooled, PPM focused high band TWT.

This program is intended to finish development of this tube in time for current and next generation system use and to establish two sources for the device. To achieve this objective, the resources of Raytheon and a subcontractor (Northrop) are being employed in a cooperative development program.

The statement of work for this program is Raytheon proposal No. PRP-4430-1 entitled "Technical Proposal for a Dual Beam Dual Mode TWT", dated 8 June 1978. To insure that all essential system performance factors are adequately addressed, a complete tube specification is being used: specifically, the Dual Mode Steering Committee Dual Mode TWT specification (originally released 12 September 1977) as amended by O.E.M. submissions to the system statement of work received May 1, 1978.

This program is divided into 4 major subtasks. The first, critical component verification, includes evaluation of means to:

1. Increase tube power output

2. Increase tube overall efficiency

3. Improve gain and power fine grain and load mismatch stability margin.

Work on these tasks is divided between Raytheon and Northrop and full transfer of information is being made between the two organizations.

2.0 TEST VEHICLES

2.1 Heat Transfer Vehicles

The following vehicles will be tested:

a) Three 3-rod units, heat shrunk.

b) Three 4-rod units, heat shrunk.

c) Three 3-rod units, brazed.

d) Three notched 3-rod units, brazed.

These units consist of four inch (101.60 mm) long CW helix sections in barrels with PPM stack, high power vacuum feed through glass viewing port, and vac-ion pump. Design of these units has been completed and parts have been ordered. Figure 2-1 shows a layout of this assembly.

2.2 Insertion Loss Vehicles

The following vehicles will be tested:

a) Three 3-rod units, heat shrunk.

b) Three notched 4-rod units, heat shrunk.

c) Three 3-rod units, brazed.

d) Three notched 3-rod units, brazed.

e) Back-to-back windows with TNC connectors.

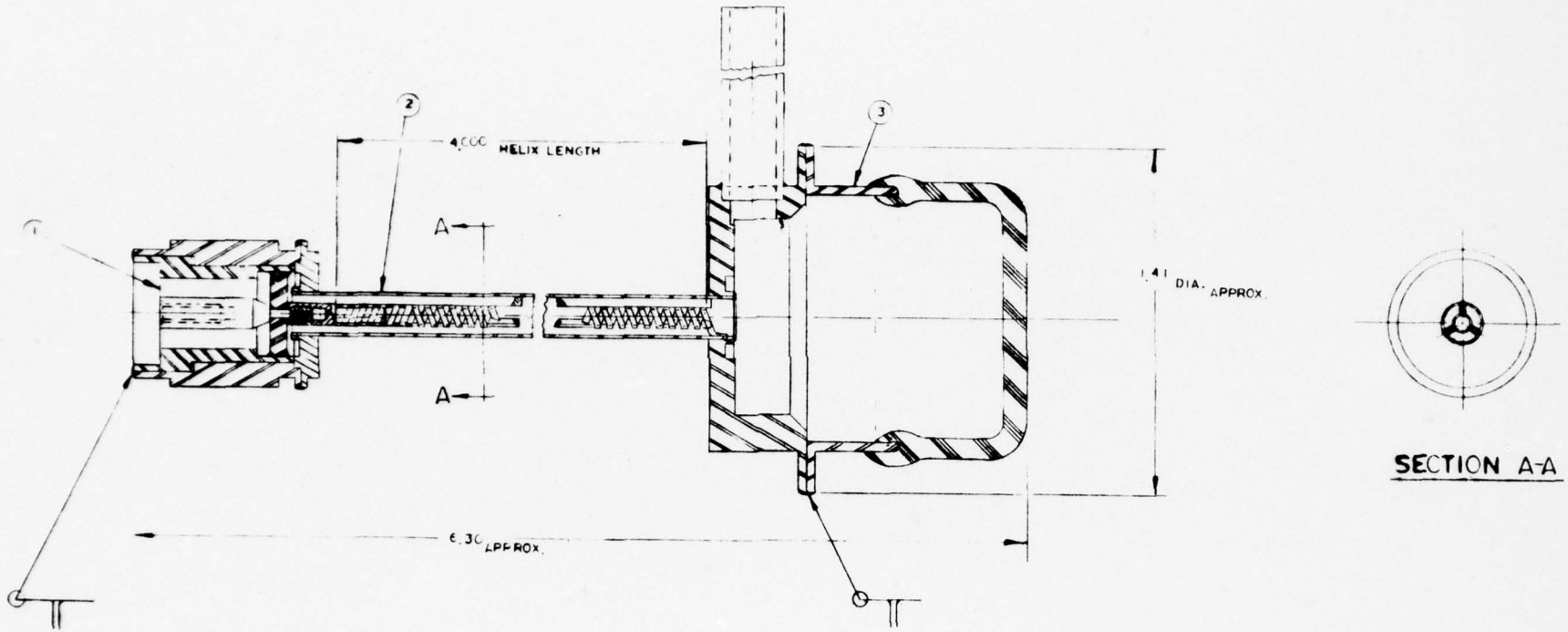

Figure 2-1. Heat Transfer Vehicle Layout.

PT-5289

These units consist of a 1.06 inch (26.92 mm) length of Pulse stage helix in a barrel with tube output windows at each end. Design of these units has been completed and parts have been ordered.

2.3 Attenuation Test Vehicles

The following vehicles will be tested:

a) Two 3-rod units, heat shrunk.

b) Two 3-rod units, brazed.

These units will consist of a CW stage output helix section with high power vacuum window and vac-ion pump. Design of these units has been completed and parts have been ordered.

3.0 HEAT SHRINK IMPROVEMENTS

Heat shrink tooling improvements have been made. In the existing design, the helix locating bars which had been added between the glue blocks had caused shifting of the rod locating bars when locking them in place. The jig has been re-designed to improve the rigidity of the glue blocks when the rod bars are locked in place by adding metal to the center of the glue blocks. The helix locking bar locking method has also been changed, from a single set screw to a swing-into-place arm which applies pressure to the bar uniformly. The result of these changes is that the entire jig has been re-designed, and that new bars have been designed to build the higher power version of the tube (CW output section and pulse stage) discussed later in this report. Two complete new fixtures (3-rod and 4-rod versions) have been designed and ordered. Delivery is expected 11-14-78.

Additional ring gauges for lapping the rod-helix assembly which will allow more precise measurement of this process, and also extend the range of interference fits to larger values, have been ordered.

Parts improvements have also been made. Rods having a reduced tolerance for the centering of the helix-mating radius have been ordered.

4.0 CW STAGE - NEW DESIGN FOR HIGHER POWER

4.1 Simulation

Figure 4-1 shows the computer model used as the baseline for computer design at higher power. Power and saturated gain data from S/N 17 are compared with the computer model. If second stage loss is taken into account, the top curve drops about 1.3 dB, bringing it within less than a dB of the actual tube value. These curves show that the computer model chosen is a good simulation of the existing tube.

4.2 Scaling for Higher Power

The baseline design (8.7 KV, 0.18A.) was scaled up to 10KV on the computer. Perveance was held nearly constant (from 0.22μP to 0.24μP) for this scale, to maintain the same focusing system. Figure 4-2 shows that increasing the perveance by 10 percent does not effect the transmission of the baseline design. Power and gain for the baseline version (8.7KV, 0.18A) and the 10KV scaled design are shown in Figure 4-3. The power has been increased by approximately 2 dB by scaling 10KV. The CW mode output power of P+1 dBm on the existing baseline design needs to be increased to meet a P+2 dBm minimum power specification. This scale should produce a nominal P+3 dBm CW mode output power, as shown on the graph.

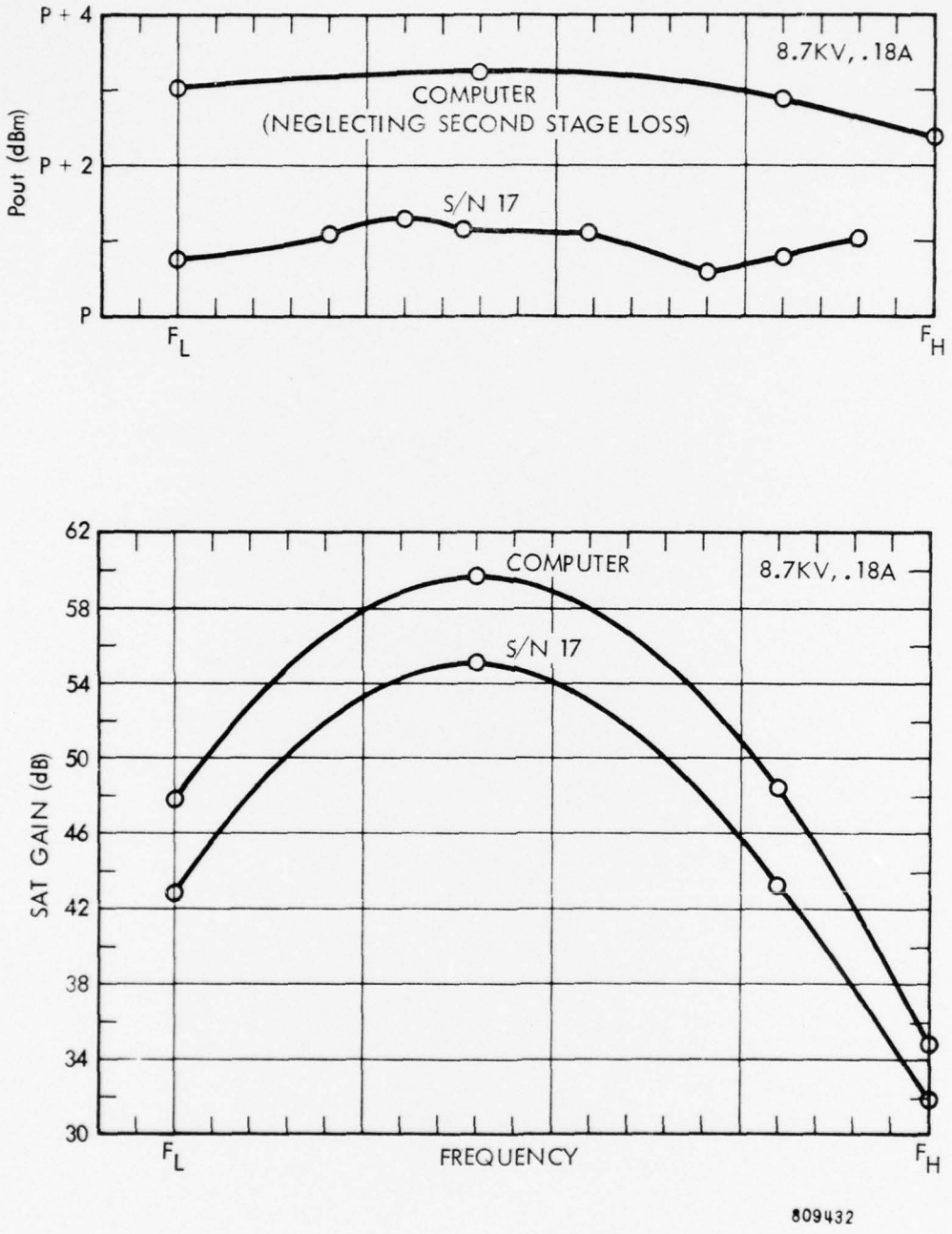

Figure 4-1. Computer Simulation of S/N 17 Power and Gain.

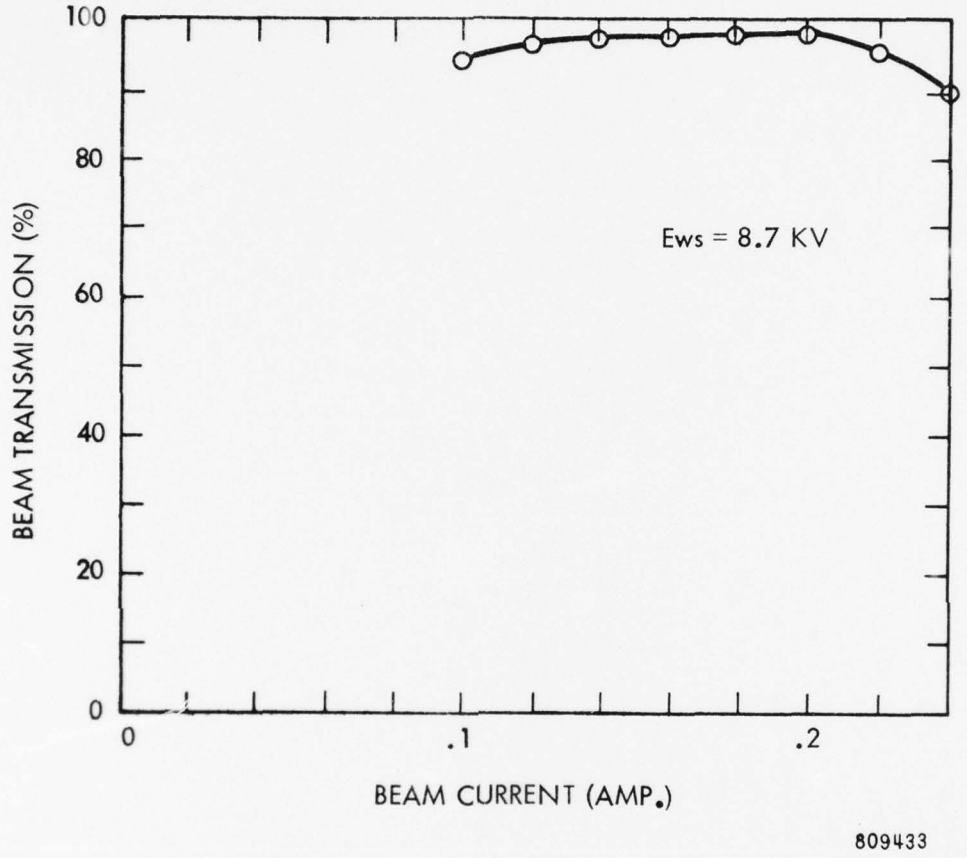

Figure 4-2. Beam Transmission vs Current CW Stage S/N 17.

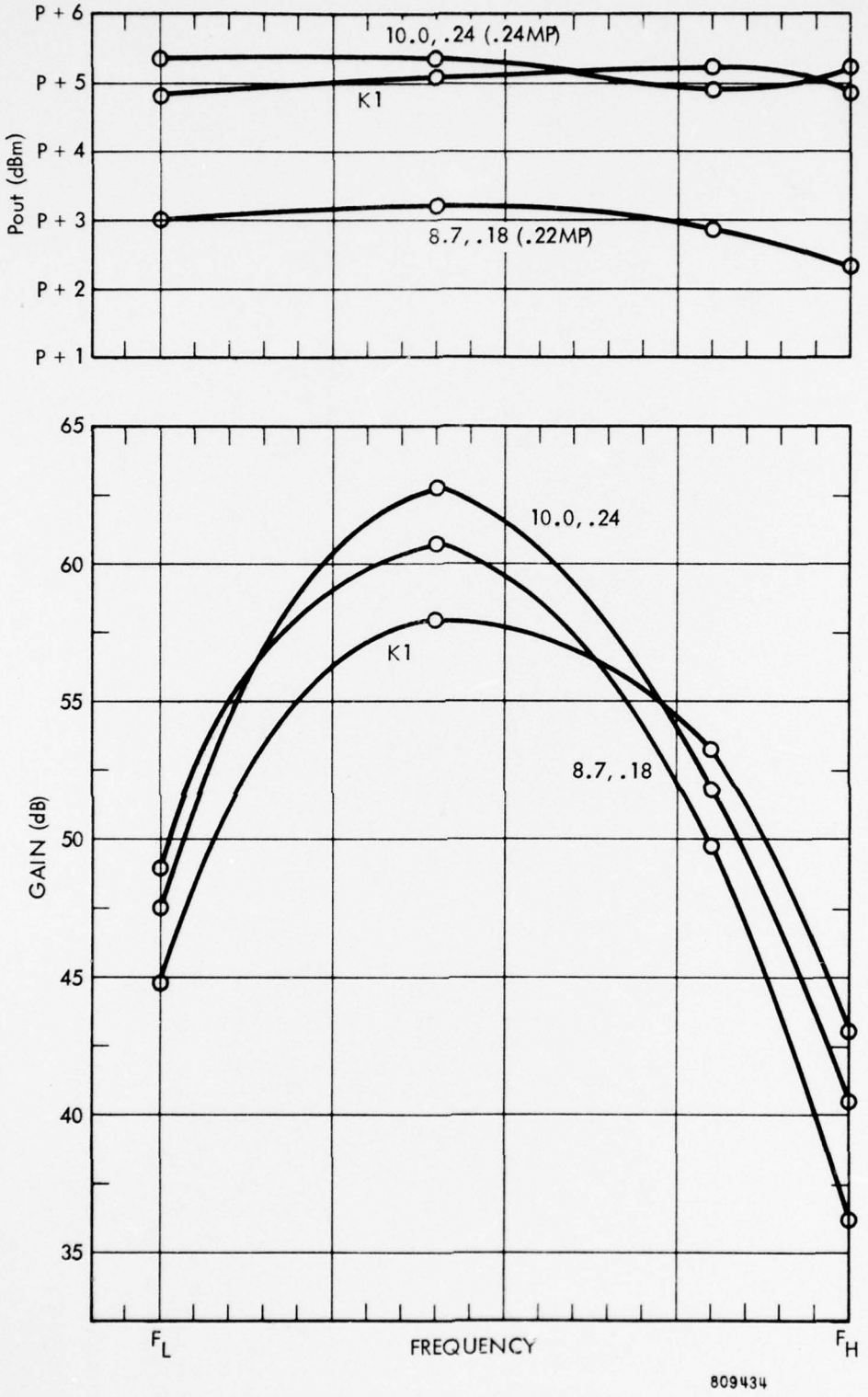

Figure 4-3. Computer Scaling - CW Stage.

4.3 Main Attenuator Shift

Output circuit analysis for oscillation threshold (discussed in more detail in a later section) has shown that output circuit gain should be reduced. To this end, the main attenuator was shifted 1.1 inches (27.94 mm) closer to the output. Figure 4-4 shows the loss pattern for the baseline and the shifted versions. This attenuator shift brought the skirt of the main attenuator up to the beginning of the buffer attenuator, which was not moved. This change is desirable in that reflections from the output side of the main attenuator will now be reduced significantly because of the presence of the buffer.

4.4 Buffer Tail Elongation

Reflections from the buffer attenuator skirt towards the output port are also a possible cause of FW oscillations in the dual tube, although measurements have shown that reflections in this area are less likely to produce oscillation than from the main attenuator. Figure 4-4 shows four skirt length variations: B, C, D, and E. In the D and E cases, the skirt extends into the velocity step in the helix, thus providing some masking of reflections from this sources. Although this source of reflection is not considered to be as important as the attenuator skirt reflections, it appeared that two objectives could be achieved at once in this change: reducing the slope of the buffer tail and masking the velocity notch.

The effects of the buffer skirt elongation are shown in Figure 4-5. Version D was chosen as the optimum tradeoff between power level and skirt length.

4.5 Input BWO

Input BWO, though not a persistant problem, had occurred occasionally at some voltage levels on recent tubes. Computer studies of the input were made and the results are shown in Figure 4-6. At 0.012 (0.305 mm) inch beam radius,

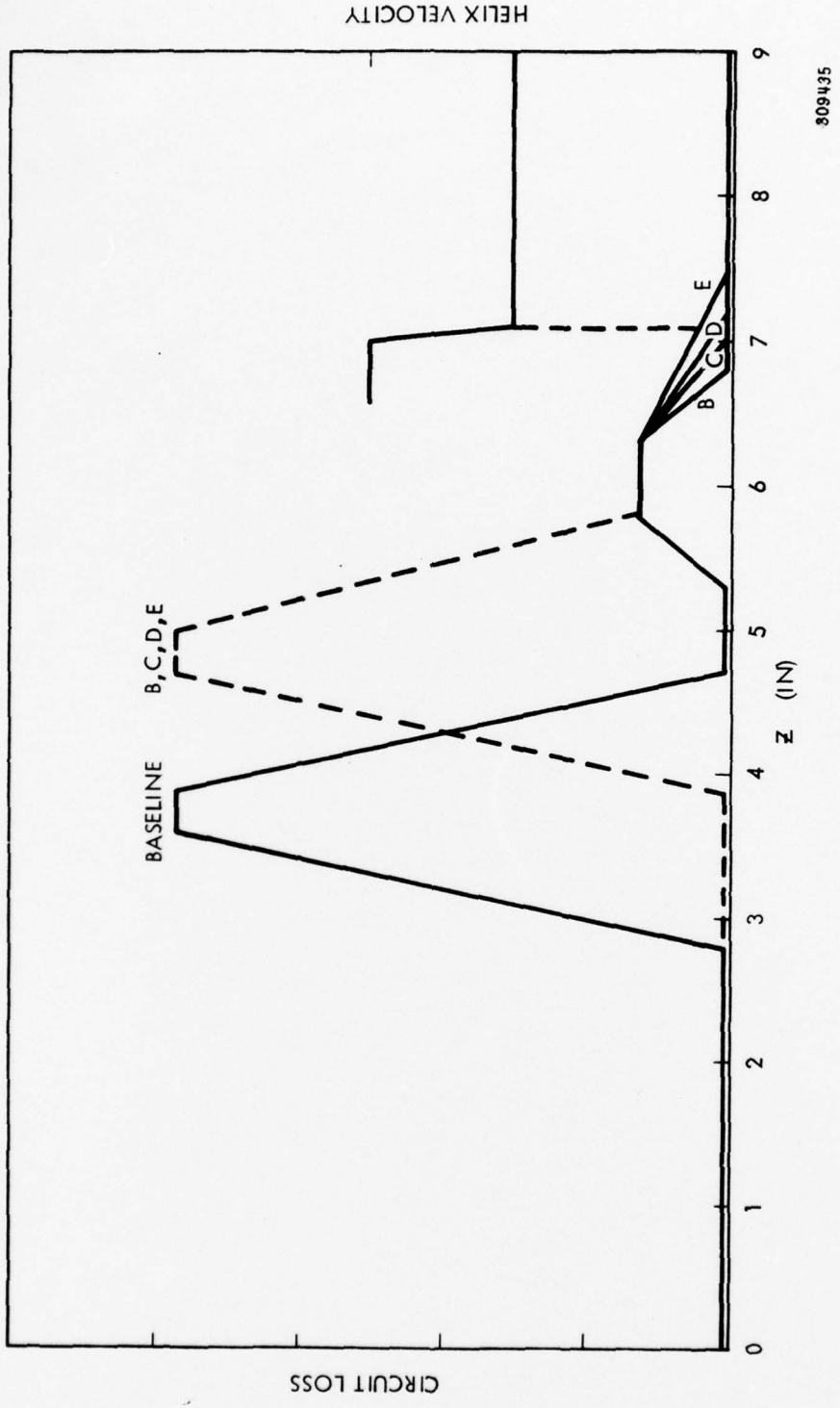

Figure 4-4. Loss Pattern - Baseline and B, C, D, E Versions CW Stage.

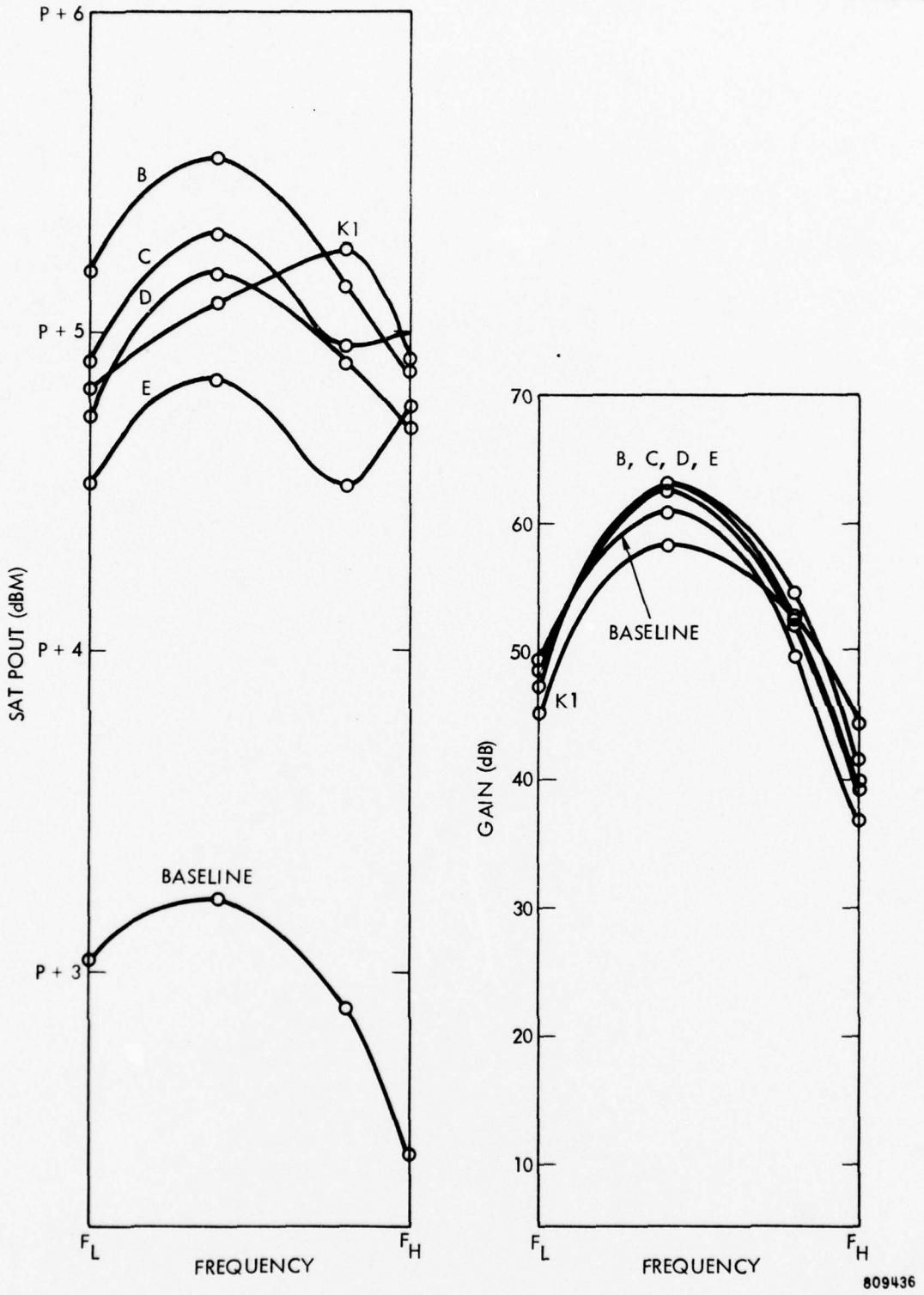

Figure 4-5. Computer Results - CW - Buffer Tail Variation.

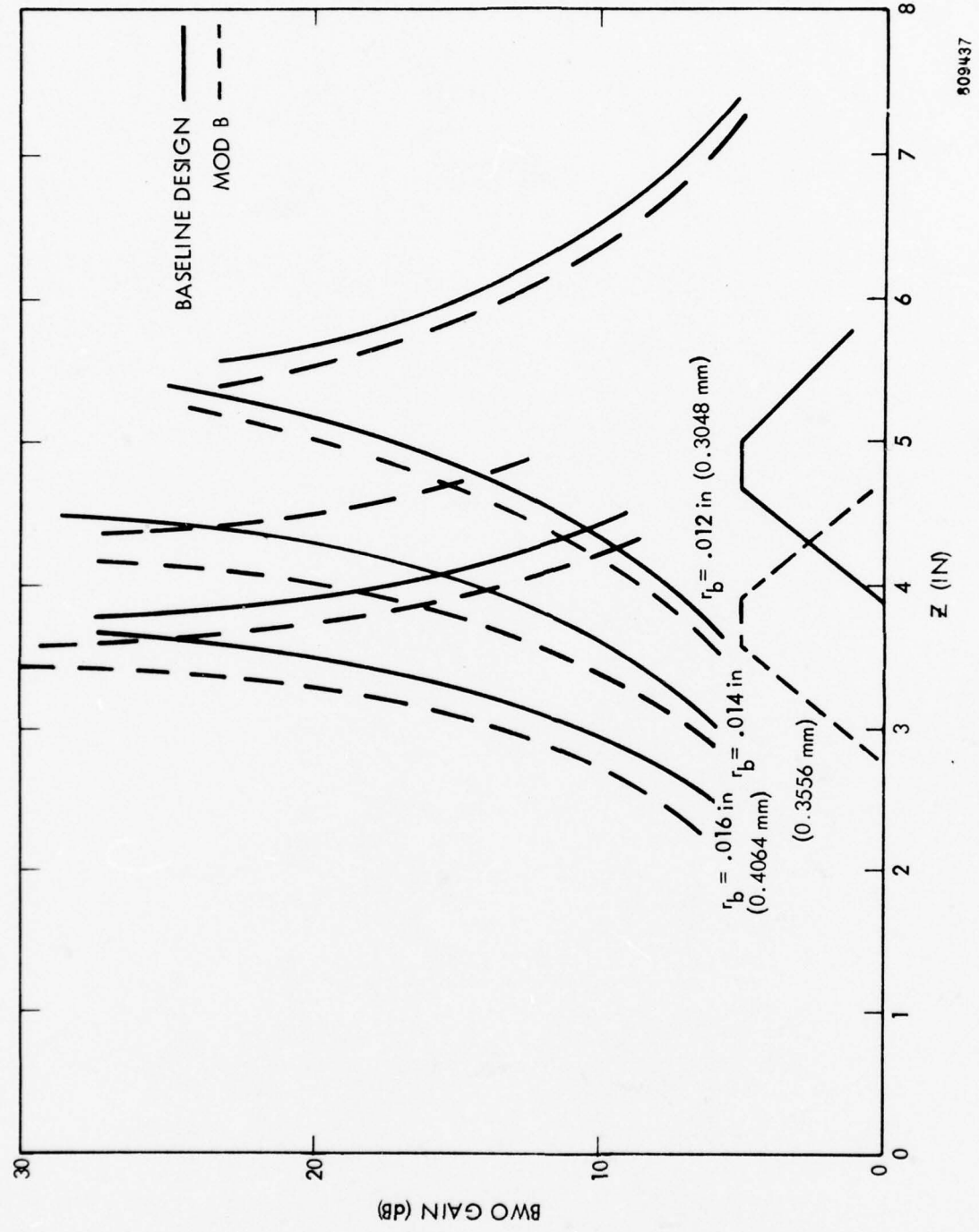

Figure 4-6. BWO Computer Data for Lossless CW Line.

the BWO peaks occur at about 5.4 inches (137.16 mm) from the input. Since the actual baseline version tubes have the main attenuator centered at 3.75 inches, (95.25 mm) some assumptions were wrong. In this case, the beam radius is probably larger, at least at the scallop peaks, which would cause the BWO peak to move back towards the input as shown on the graph (Figure 4-6), or, the computer program is not precise enough. At 0.016 inches (0.406 mm) beam radius the peak begin to move inside of the baseline main attenuator. Though the beam diameter is known not to be this big, it is desirable to have a computer analysis capability, at least on a relative basis, for input BWO.

An input pitch step was then developed, using the 0.016 inch (0.406 mm) beam model, which would move the BWO peak past the main attenuator, taking into account the new 1.1 inch (27.94 mm) shifted attenuator position. The results of this pitch step are shown in Figure 4-7. The two peaks (one for each helix velocity section) are shown, both to the right of the main attenuator. This design, including all of the changes discussed in this and previous sections, is version K1.

4.6 Design Version K1

Figure 4-8 shows the expected (corrected for computer model deviation from measured data, i.e. "Real") saturated power output and gain for the design thus for, namely version K1. Power output is approximately P+3 dBm and gain is well centered across the band.

Attempts to design an equalizer for the K1 version were unsuccessful, however. An equalizer which levels the gain at rated operating point causes a droop in small signal gain, as shown in Figure 4-9, at the high band edge. The reason for this problem is shown in Figure 4-10, where it is seen that the SSG comes much closer to the saturated gain at the high band edge than elsewhere in the band for K1 version.

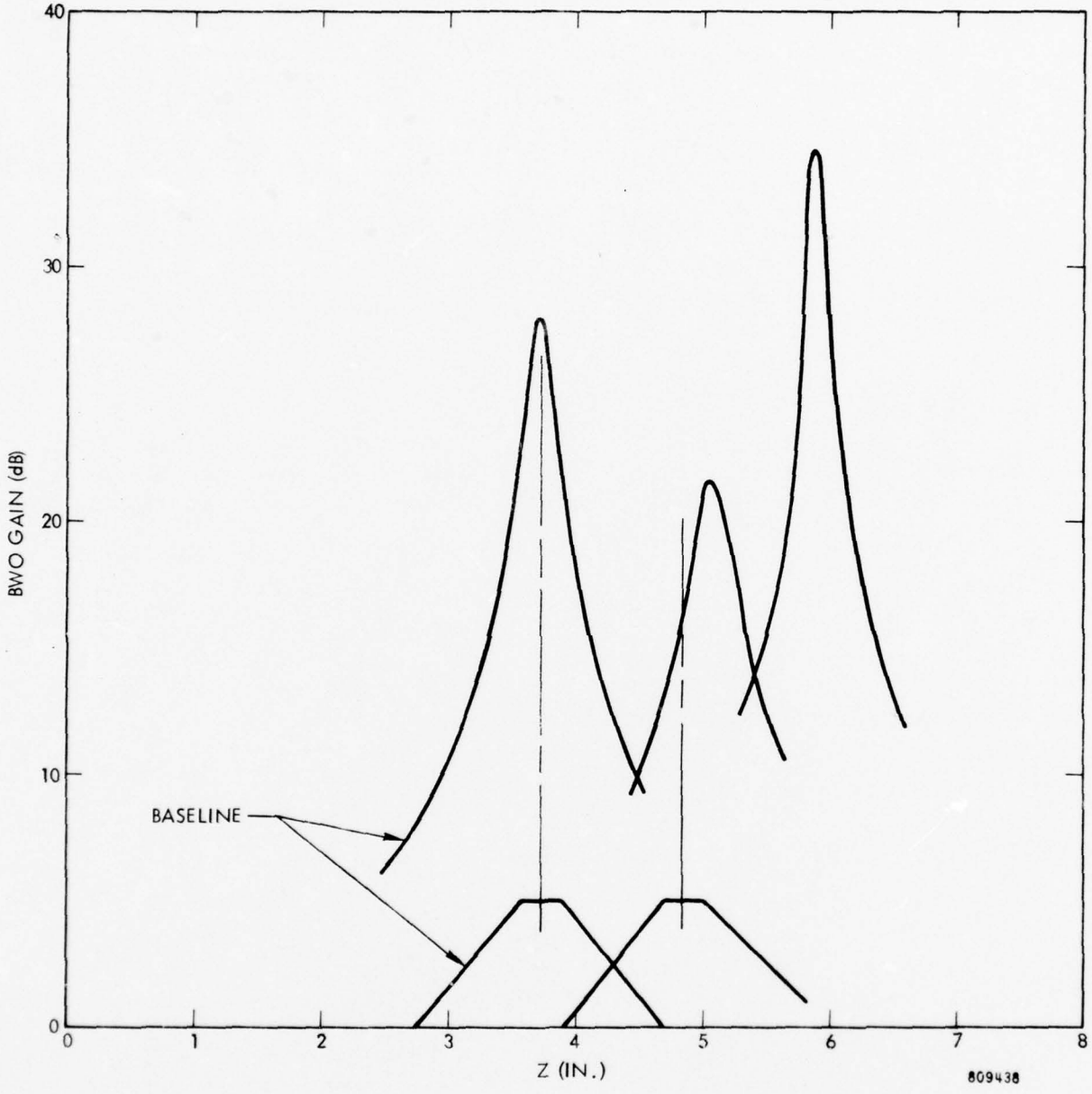

Figure 4-7. BWO Computer Data for Lossless Lines - K1 Version vs Baseline.

PT-5289

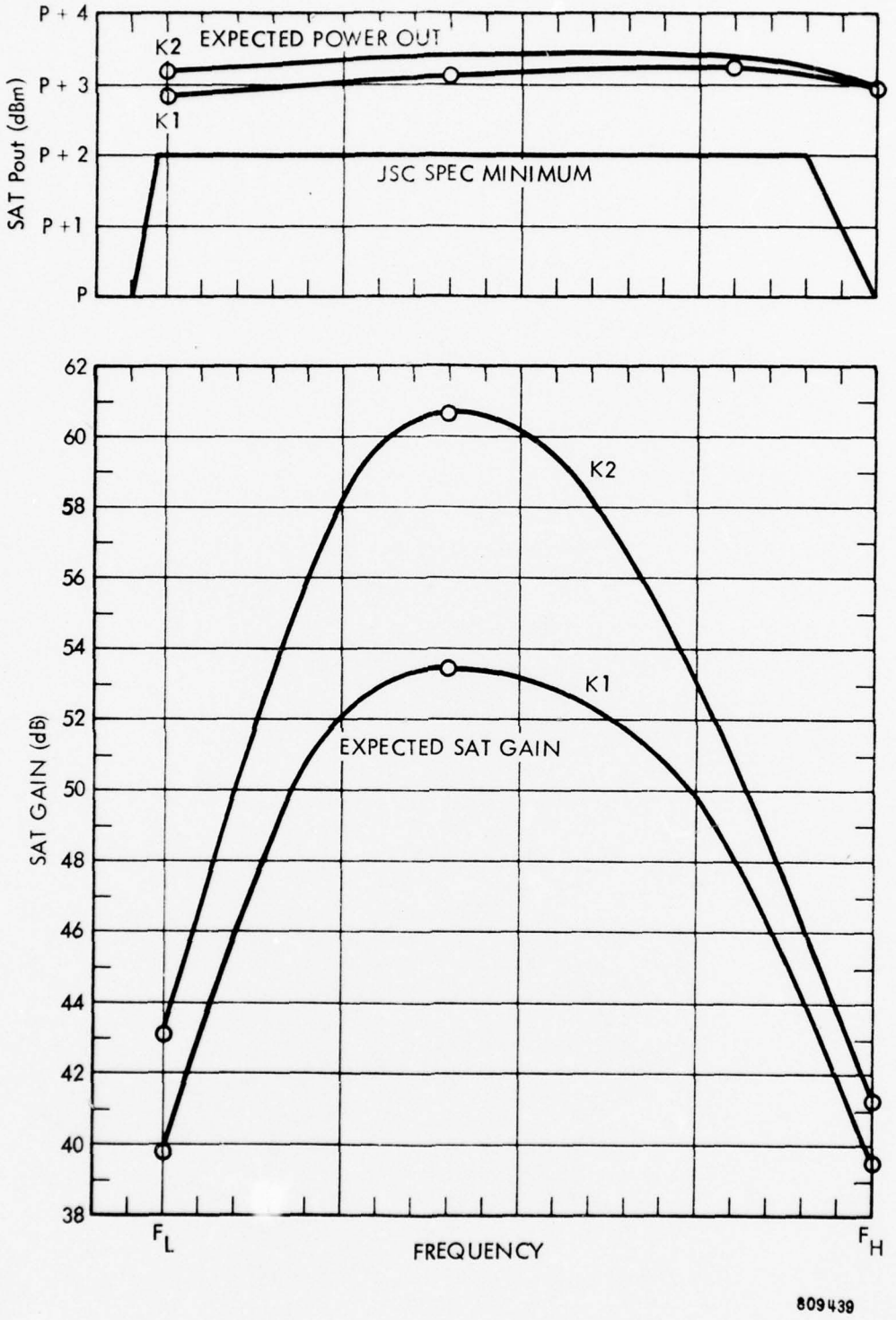

Figure 4-8. Expected Performance - SIM K1, K2.

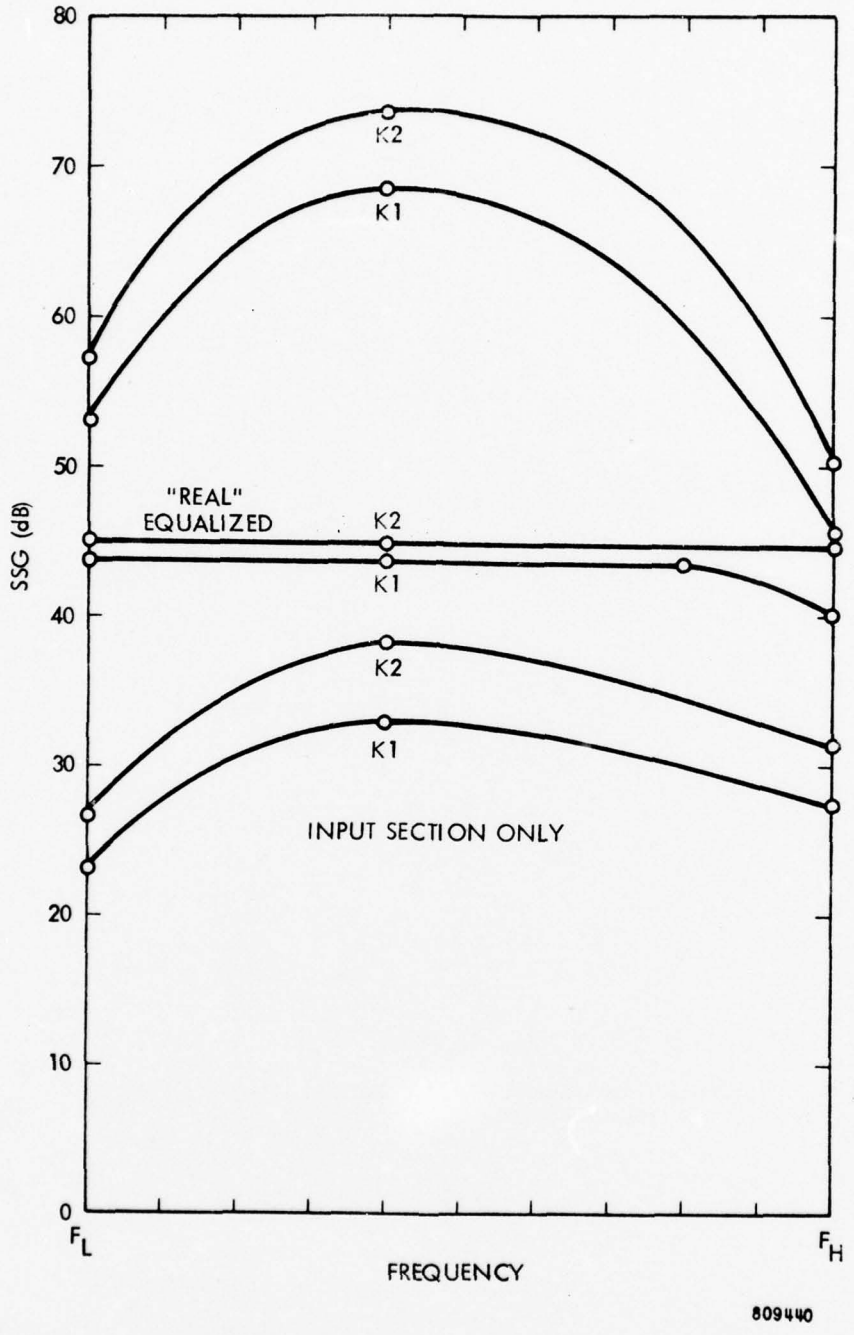

Figure 4-9. Small Signal Gain K1 and K2 Versions.

PT-5289

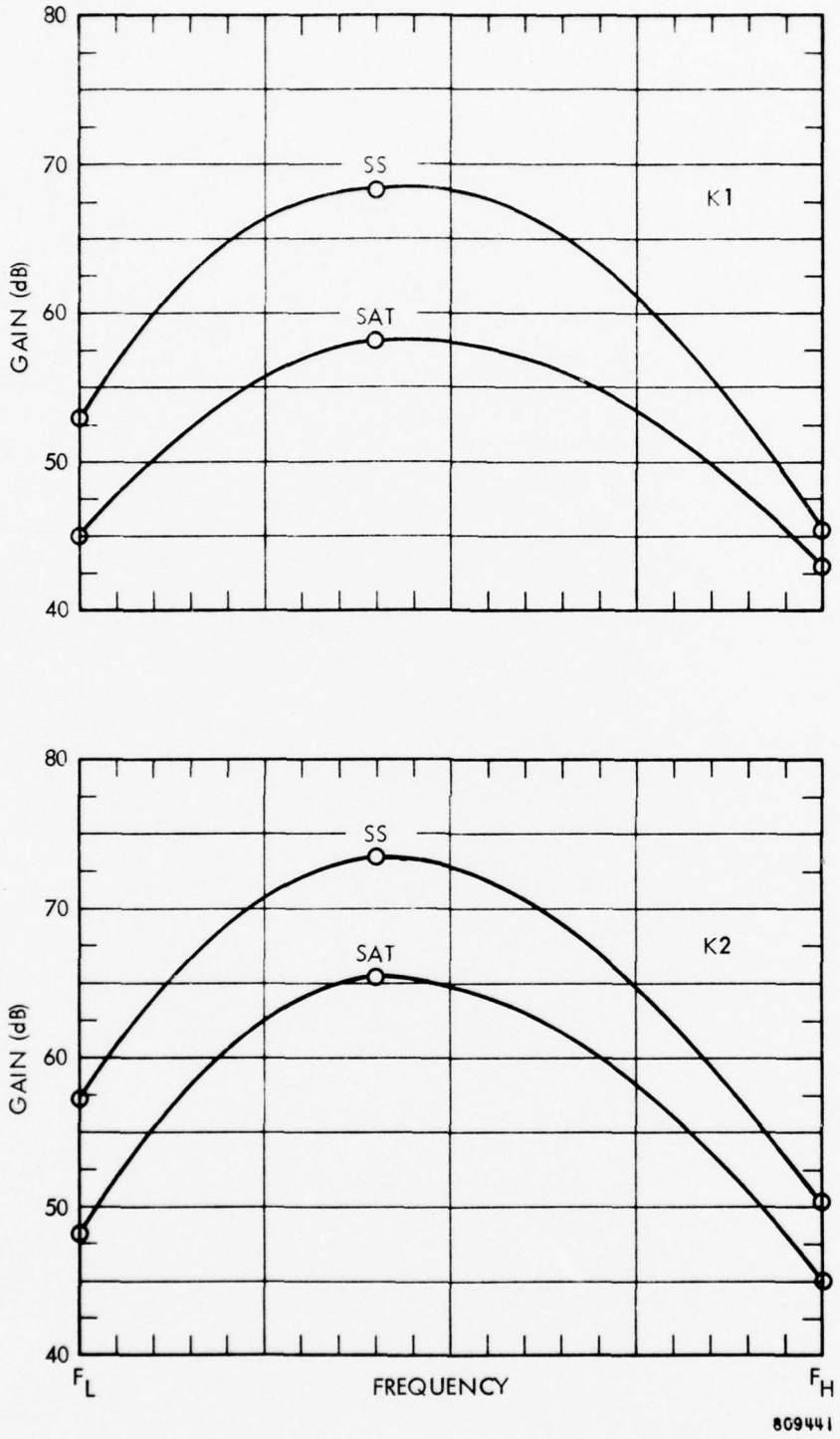

Figure 4-10. Gain Comparison, K1 vs K2 Versions.

4.7 Design Version K2 - Reduced Input Helix Diameter

The input section helix was then reduced in diameter by 0.004 inches (from 0.077 to 0.073 inches) (1.956 mm to 1.854 mm) and the input helix pitch adjusted to maintain constant velocity. The input helix pitch step was omitted at this time - other BWO suppression techniques will be discussed below. Version K2 shows a marked difference in SSG at the high band edge, as seen in Figure 4-10, compared to K1 version. The effect of this change was to increase the gain gain of the tube at all frequencies (due to the increased beam fill factor) as well as to improve the SSG to saturated gain separation at the high band edge. The equalizer calculation for this version results in level SSG, as seen in Figure 4-9. Saturated gain was also increased, as seen in Figure 4-11, although not as much as the SSG, particularly at the high band edge.

The effect on power output of the input helix diameter reduction is shown in Figure 4-8 on a corrected (expected or "real") basis, relative to version K1.

4.8 Input Buffer Attenuator

The input helix diameter reduction introduced in K2 version increased the small signal gain of the input section. The helix velocity step in the input was omitted at that time because it was known that further BWO suppression was not possible with a velocity step (without serious tradeoffs of gain or power), and that the FW gain was now becoming large enough to require some attention to prevent FW oscillations.

A 10 dB buffer attenuator was added to the input section to prevent FW and BW oscillation. The loss and velocity pattern for this change is shown in Figure 4-12. The 10 dB buffer caused a 3.5 dB decrease in FW small signal gain at mid-band, which in turn required an extra 0.3 inch (7.6 mm) length of

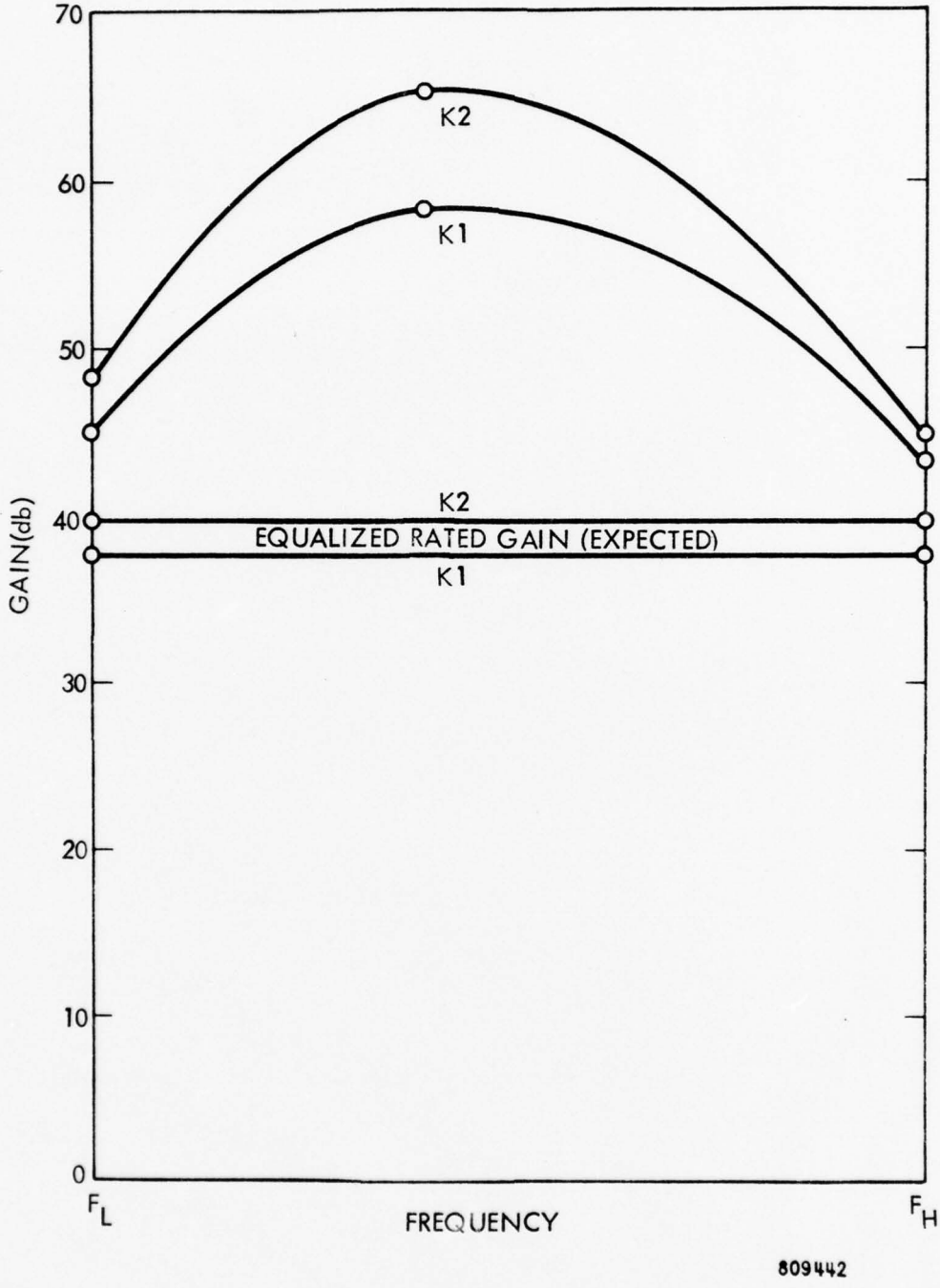

Figure 4-11. Saturated Gain.

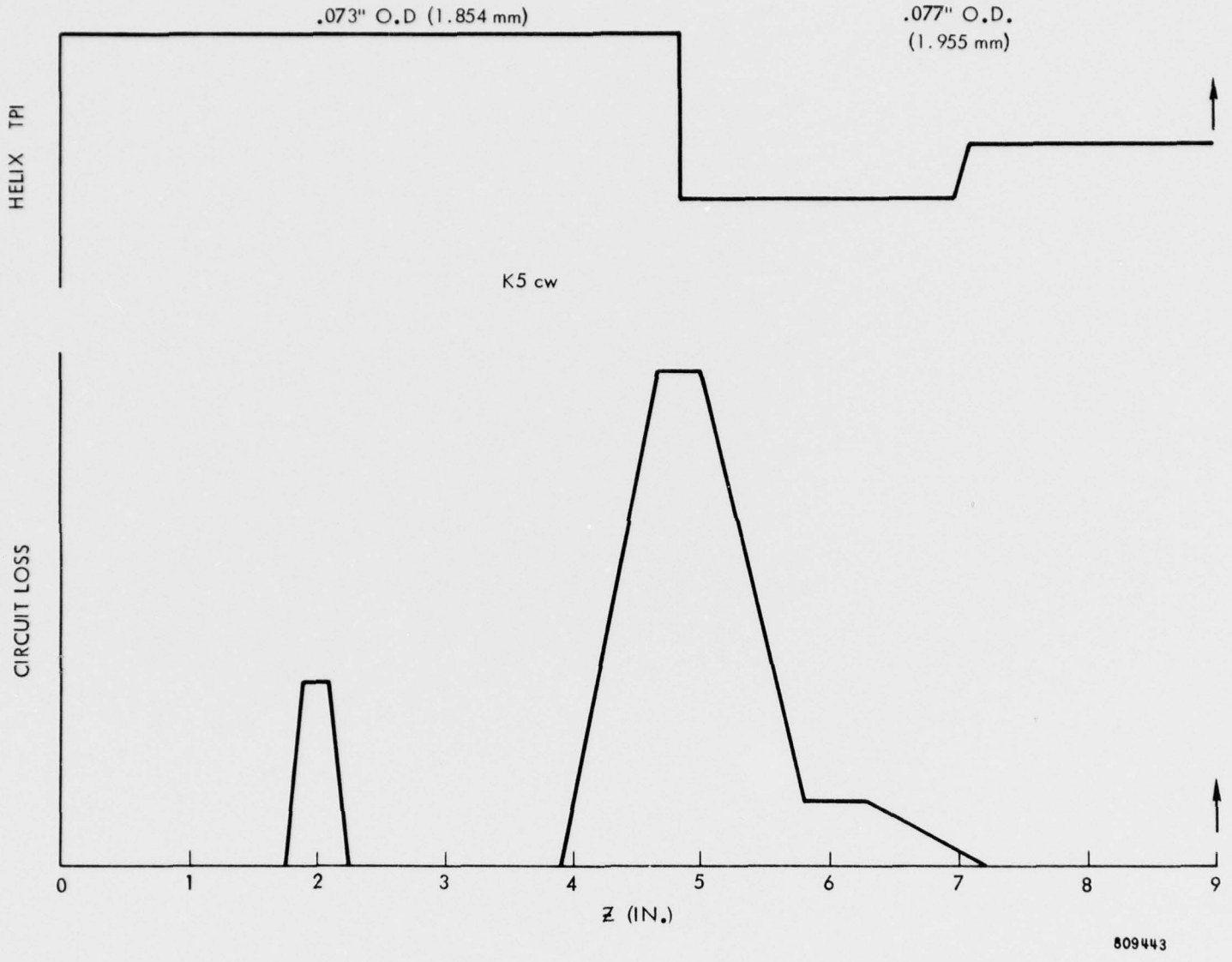

Figure 4-12. Circuit Loss and Velocity vs Distance - K5 Version.

input helix section to restore this gain, bringing the circuit length up to 9.3 inches. (236.22 mm) Packaging considerations indicate that the extra tube length is available.

Figure 4-13 shows the circut loss and velocity patterns for the 9.3 inch length version, K16. The addition of 0.3 inches to the input restored the 3.5 dB of SS gain at midband and restored the power and gain of the tube to that given for version K2.

4.9 Input Oscillation Threshold Analysis

An analysis of the FW and BW oscillation thresholds for version K16 is given in Figure 4-14. It assumes worst case input reflection (3/1 VSWR vs a probable 2.5/1 specification value, and 2/1 tube reflection vs a probable 1.6/1 VSWR) and worst phase of the tube and external reflections, for a 6.0/1 VSWR total.

The effect of the 10 dB buffer increases the main attenuator skirt relection threshold from 1.053 to 1.147 VSWR, a very comfortable margin of safety for FW oscillations.

The BW analysis uses only one-way loss, even though the gain figure used was computed for a lossless helix. The 1.42 VSWR threshold is therefore a very conservative estimate, indicating that BWO would be impossible.

5.0 COMPUTER MODEL OF CHAIN

A computer model of the chain has been written. It uses the output section of the CW stage, its bridge, and the pulse stage.

The oscillation loops included in the program are detailed in Figure 5-1. Version 1 computes the oscillation loop gain or the threshold VSWR, depending on whether or not the notch and main attenuator VSWR are given as input or left

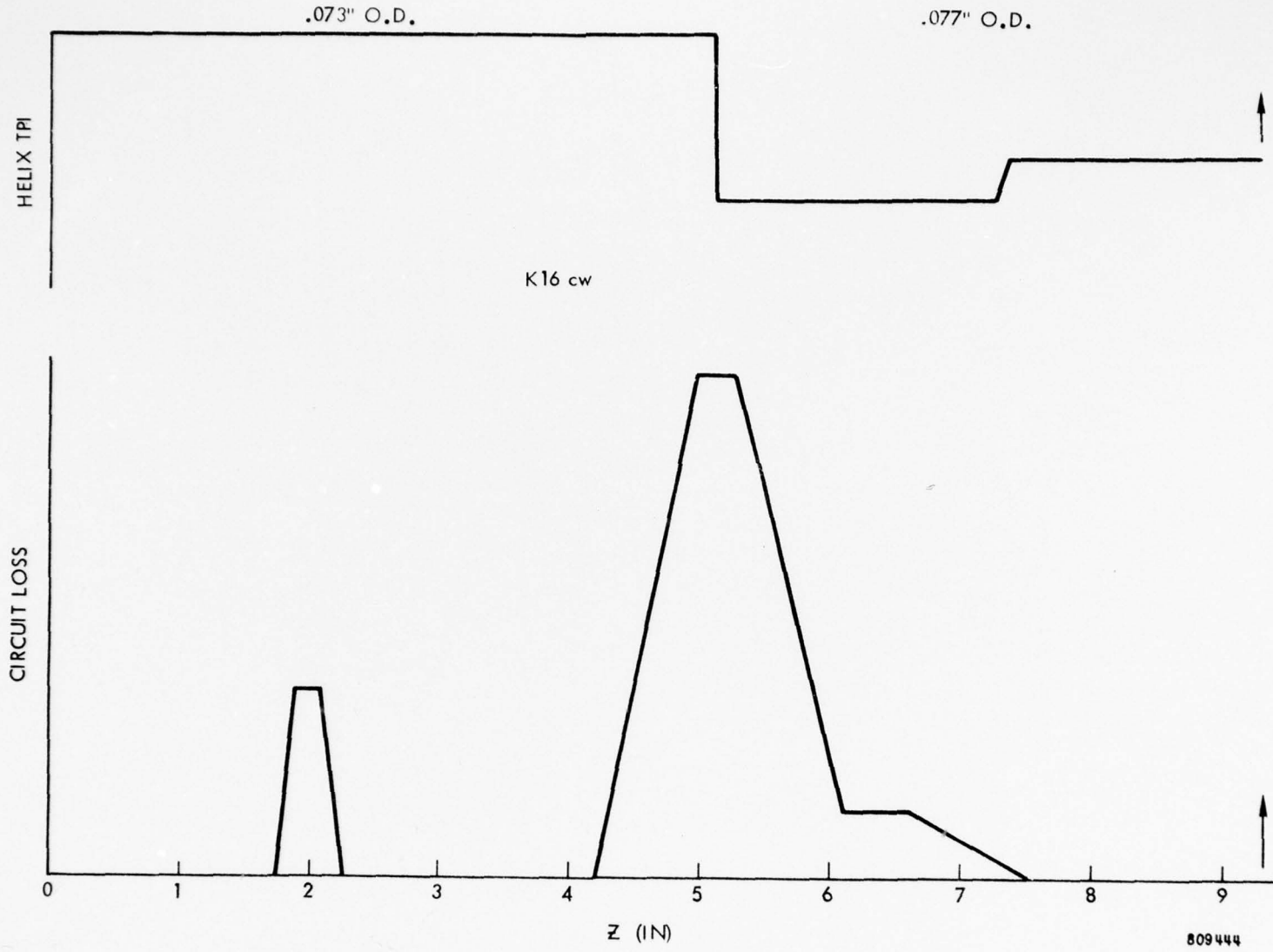

Figure 4-13. Circuit Loss and Velocity vs Distance - K16 Version.

FIGURE 4-14

INPUT CIRCUIT OSCILLATION - CW STAGE - K16

TUBE INPUT VSWR = 2.0/1
INPUT LOAD VSWR = 3.0/1
WORST INPUT VSWR = 6.0/1

F.W. OSCILLATION

GAIN = 38.2dB
LOSS ≅ -2.dB
INPUT REFLECTION LOSS = -2.9dB (6.0/1 VSWR)
MAIN ATT. VSWR FOR OSC. = 1.053 (-33.3dB GAIN)
ADD 10dB LOSS:
MAIN ATT. VSWR FOR OSC = 1.147 (-23.3dB GAIN)

B.W. OSCILLATION

GAIN = +30dB
LOSS ≅ 2dB
INPUT REFLECTION LOSS = 2.9dB (6.0/1 VSWR)
MAIN ATT. VSWR FOR OSC. = 1.11B (-25.1dB GAIN)
ADD 10dB LOSS (NEGLECTING FORWARD LOSS):
MAIN ATT. VSWR FOR OSC. = 1.42 (-15.1dB GAIN)

VERSION 1

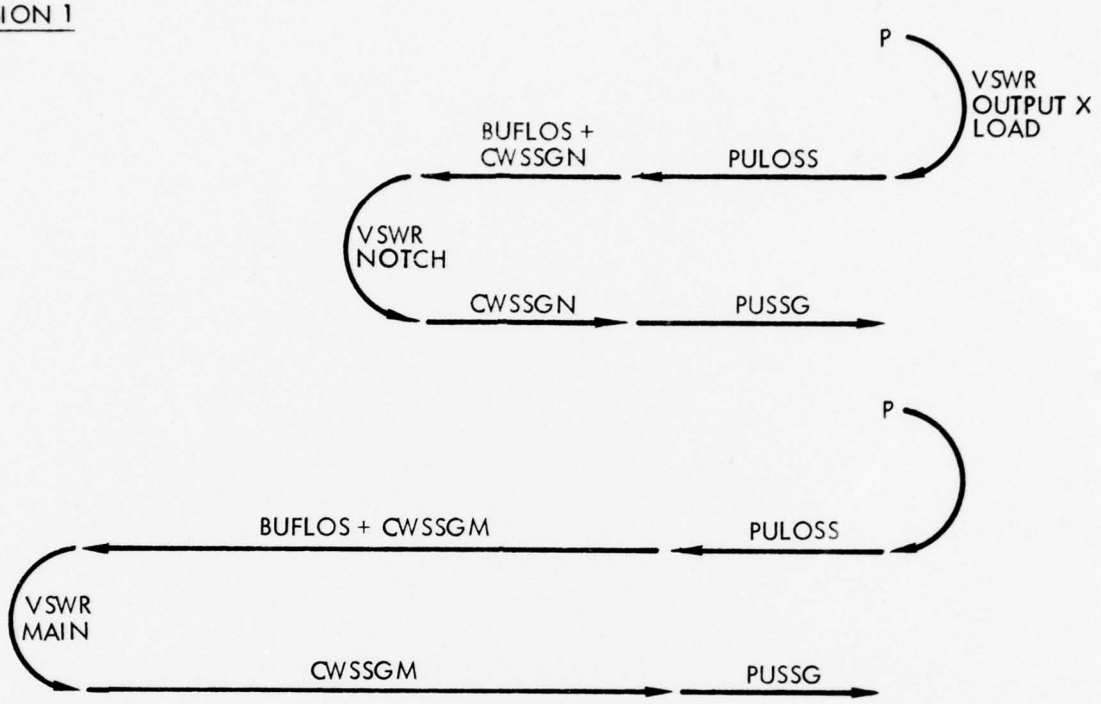

VERSION 2

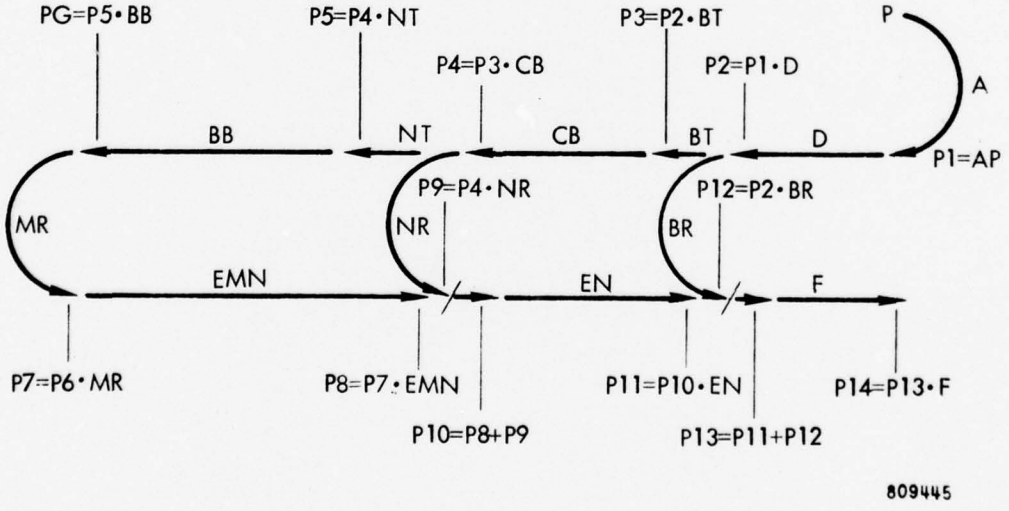

Figure 5-1. Oscillation Threshold Computer Program Layout.

out. Both loops shown in Version 1 are computed simultaneously. The upper loop considers only the effect of a reflection at the helix notch (or buffer skirt) region and the second loop considers only the effect of the main attenuator VSWR, as if each existed independently. This model enables us to determine the worst case for these loops, since they assume that all output reflected power arrives unscathed at the reflection in question - a highly improbable worst case.

Version 2 of the program, which can be called by a single added input option, is the more general case. It accepts reflections from the bridge, notch-buffer area, and main attenuator skirt as input data, for each iteration, and calculates the loop gain for that combination.

Version 2 begins with an assumed value of power arriving at the output of the pulse stage. This power is reduced by A, for load and tube reflections combined, then attenuated by D, the pulse stage loss. This power level, P2, is then split into two components: the power reflected from bridge area reflection, P12(which is added to the forward power arriving at the bridge) and the power remaining, P3, which is attenuated by the loss in the last part of the CW stage, CB. This power level, P4, is then split into two components: the power reflected from the notch-buffer area, P9 (which is added to the forward power arriving at the notch buffer area), and the power remaining, P5, which is attenuated by the loss of the buffer attenuator and the middle helix section. This power level, P6, is then reduced by the reflection coefficient of the main attenuator to P7, and then sent along the circuit as injected forward signal, where the small signal gain of the three sections, as well as the reflected signals, P9 and P12, are applied as they occur. The resultant level, P14, is compared to the initial power, P, and the loop gain is established.

Using Version 2, some values of bridge reflection thresholds were calculated: for a 1.001 VSWR at the main attenuator and also at the notch-buffer area (essentially no reflection), the bridge threshold is 1.75/1 VSWR, for a 3/1 output load VSWR and a 2/1 tube output VSWR at worst phase, namely,

6.0/1 net output VSWR. This shows that the bridge reflections, which are always below 1.5/1 VSWR, cannot cause the second stage to oscillate at any drive level.

It should be noted that these computer programs neglect phase shift. This limits their usefulness to modelling which assumes that all reflections always return in proper phase for maximum addition of signals. This worst-case approach is justifiable because the wide bandwidth of this tube will permit proper phase to exist at some place in the band. However, oscillation depends upon being in the highest small signal gain region of that band. It is possible then, that the necessary phase and gain conditions will not co-exist, even when the program indicates oscillation conditions.

6.0 SEPARATE POWER SUPPLIES TESTING

Second stage power output in the baseline design falls off at the upper band edge at about F_H-2 (See Figure 6-1). Since all testing had been done with E_{ws} optimized for CW mode operation, it was felt that the pulse stage was not perfectly optimized for beam voltage. Before computer modelling for higher power was begun, it was necessary to determine the optimum E_{ws} for the pulse stage so an accurate simulation could be established.

The dual mode test set was modified to allow operation at separate voltage for each stage. Gain curves were taken at various beam voltages, as shown in Figure 6-2. From this curve it is seen that the optimum voltage is near 8.5 KV. Figure 6-3 shows the power and pulse-up gain at this voltage. The conclusion from this test is that the pulse stage was being operated 150-200 volts too high, and that high-end power drop is much less pronounced when voltage is corrected, i.e., the second stage has more bandwidth than it had appeared to have at constant voltage conditions.

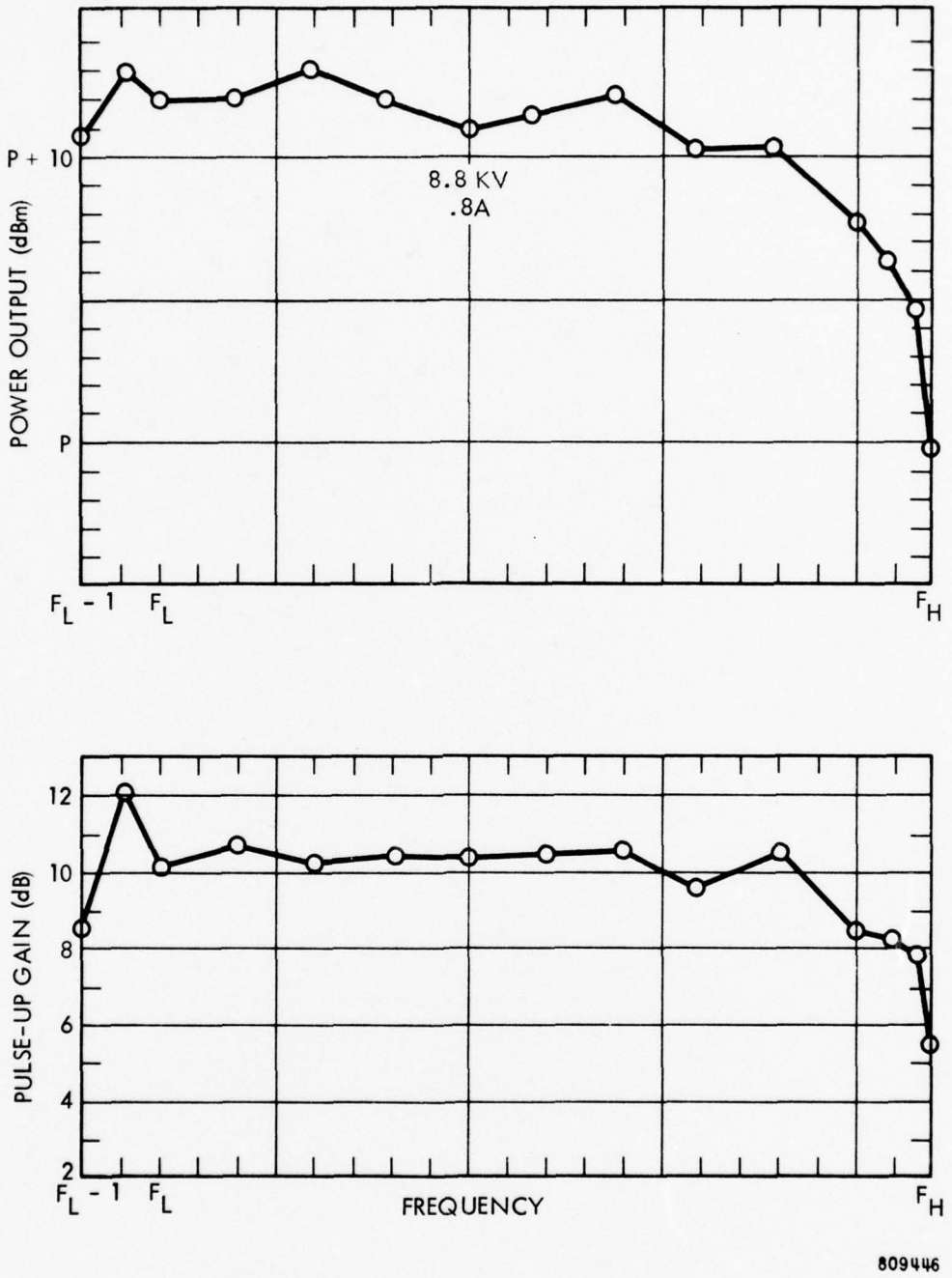

Figure 6-1. S/N 17 Single Voltage Test Pulse Stage.

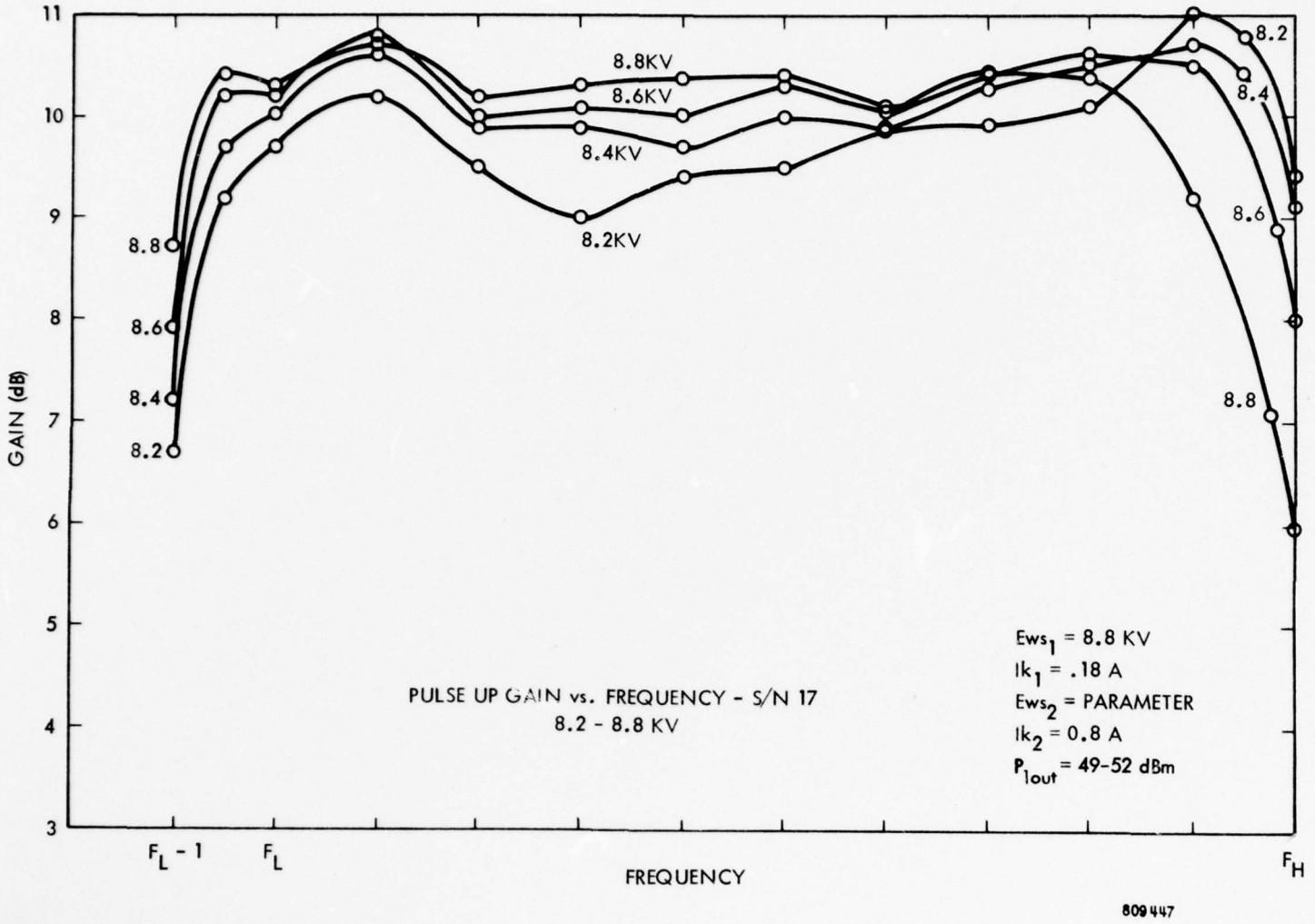

Figure 6-2. Pulse Stage Voltage Variation - S/N 17.

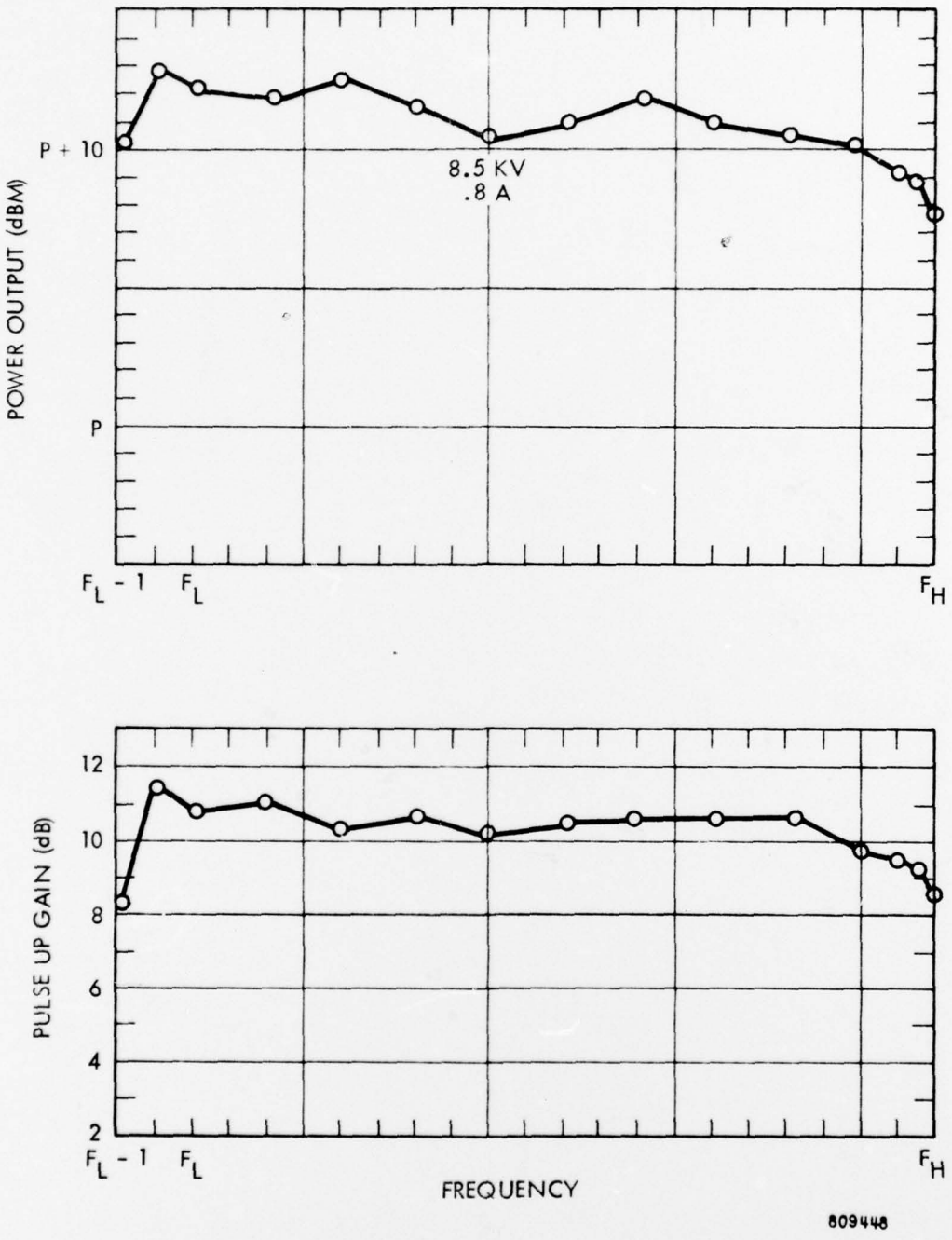

Figure 6-3. S/N 17 Dual Voltage Test.

7.0 PULSE STAGE - NEW DESIGN FOR HIGHER POWER

7.1 Computer Model of Pulse Stage

Before the second stage design could be modified for higher power output, an accurate computer model was required. The existing model was not a close enough fit to the observed data.

Drive power limitations are an important factor in second stage testing: since the maximum power output of the first stage is limited, complete transfer curves into the overdrive region cannot always be taken. It is expedient to base the simulation on matching the test results in the small signal region as well in the operate region to insure a good overall match of the transfer curves. Towards this end, data is shown for two points on the transfer curve; P-10 dBm drive, in the small signal region, and P dBm drive, in the rated operate region.

Figure 7-1 is the power output at P dBm drive vs frequency for the most recent tube, S/N 17, compared to the computer model which was established during this program. The match is excellent.

Figure 7-2 is the power output at P-10 dBm drive vs frequency for S/N 17 compared to the new computer model. When the S/N 17 curve is dropped by 1 dB (dashed line) the agreement between computer model and tube data is excellent. The reason for the 1 dB reduction is that the loss of the second stage must be considered in determining actual second stop drive. The actual drive to the second stage is at least 1dB higher than the power measured at the output port. Since the tube transfer function is linear in the SSG region, this adjustment can be taken in the power output curve or the power input curve in order to correct for its impact on gain.

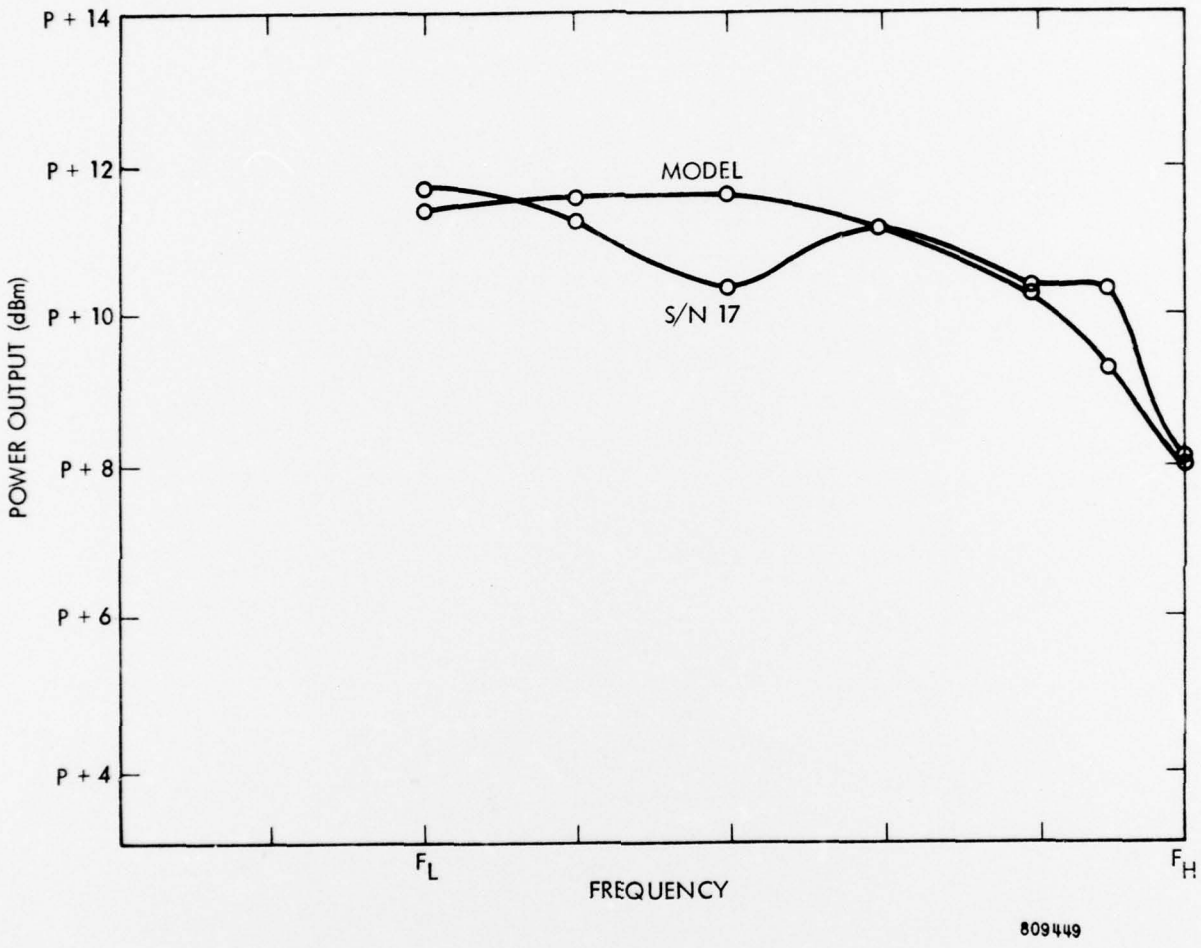

Figure 7-1. Power Output Pdbm at Watts Drive S/N 17 vs Model.

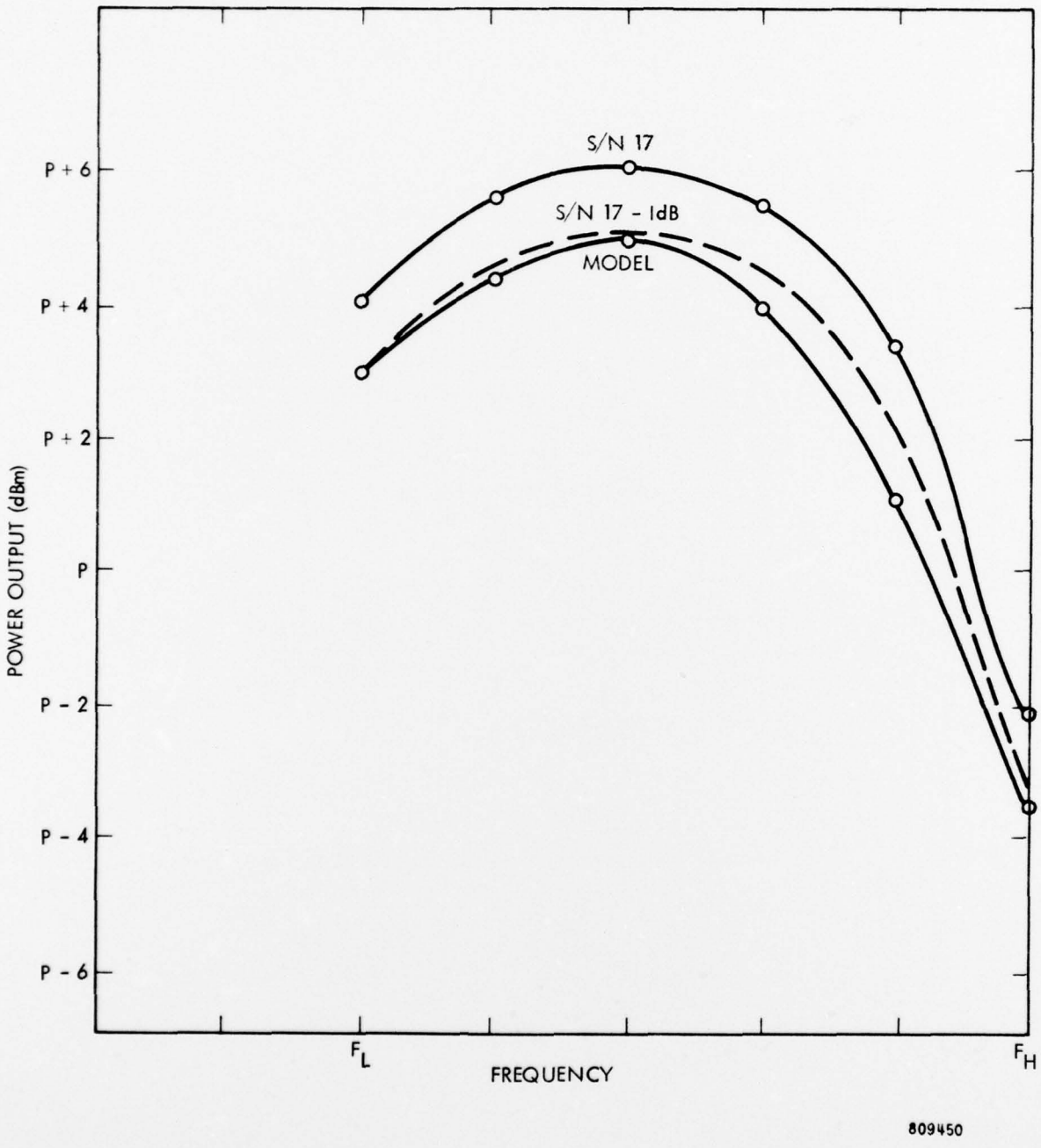

Figure 7-2. Power Output at P-10 Watt Drive S/N 17 vs Model.

7.2 Pulse Stage CAD

Some computer design work has been done using the computer model described in the previous section. The gain of a 10KV scaled up version has been computed, and is shown in Figure 7-3. Gain is plotted for two drive levels. The rated curve shows that the 10 dB pulse up requirement is met at all frequencies except F_H-.1 to F_H, and the small signal curve shows excessive drop off at the high end of the band. Further work will be done to correct these deficiences.

8.0 COAX-TO-WAVEGUIDE TRANSITION

A three stage impedance transformer from WRD750-D24 waveguide to reduced height 50 ohm double-ridged waveguide which preserves guide wavelength and TE20 cutoff frequency has been developed, and a back-to-back transition built and tested. The results, shown in Figure 8-1, except for the very low band-edge, are considered excellent. Matching of coax into waveguide currently is progressing with the three stage transformer while a new 6 stage transformer has been designed in an attempt to improve band-edge VSWR.

Match work in the coax transition region has been carried out: three runs were made using different coax insert sleeve lengths. The results of these runs were somewhat inconsistant, leading to an investigation of the coax (SMA) connector being used. Tests were made from waveguide into coax load and from coax into waveguide load, through the transition (See Figure 8-2). These tests showed that the SMA connector was not suitable for this task. Precision type-N connectors were then ordered for replacement and will be used for further transition match testing.

9.0 DUAL STAGE COLLECTOR DESIGN

A dual stage beam collector preliminary layout has been completed. To achieve maximum internal volume for good radial beam spread, and lowest part count, a cylindrical geometry was chosen. Each collector stage is a pre-brazed

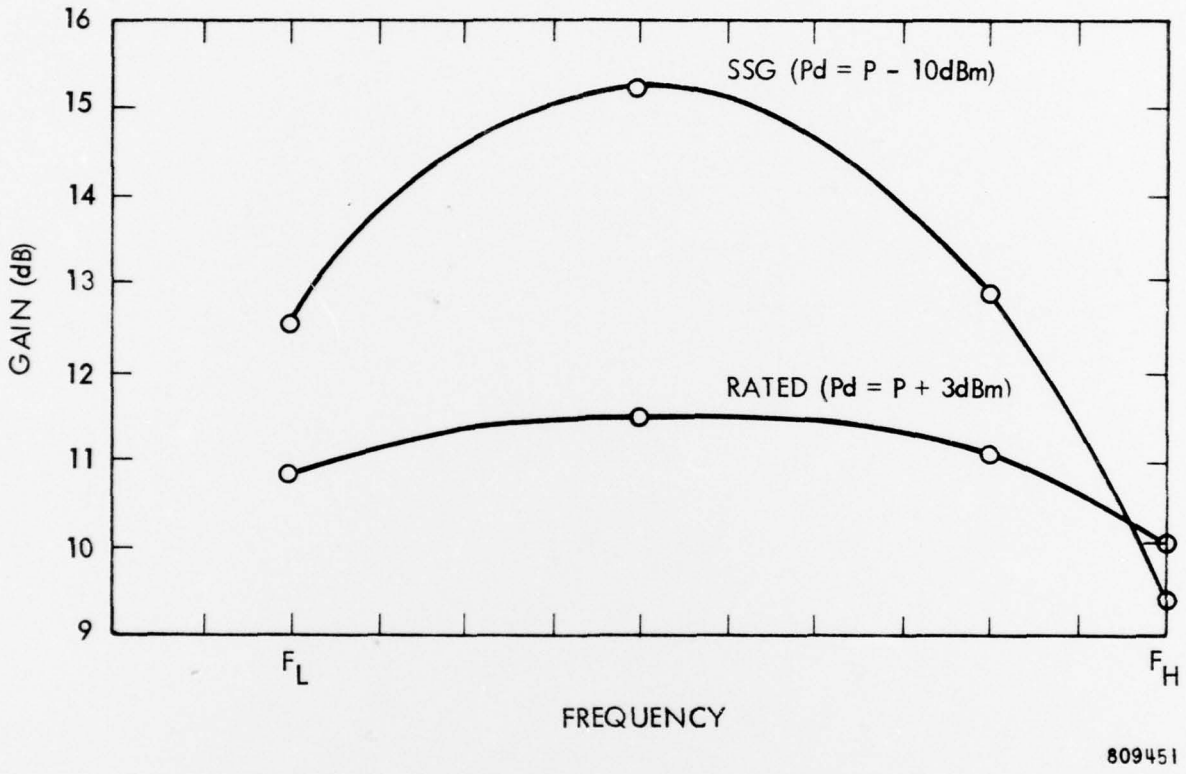

Figure 7-3. Pulse Mode Gain - L61.

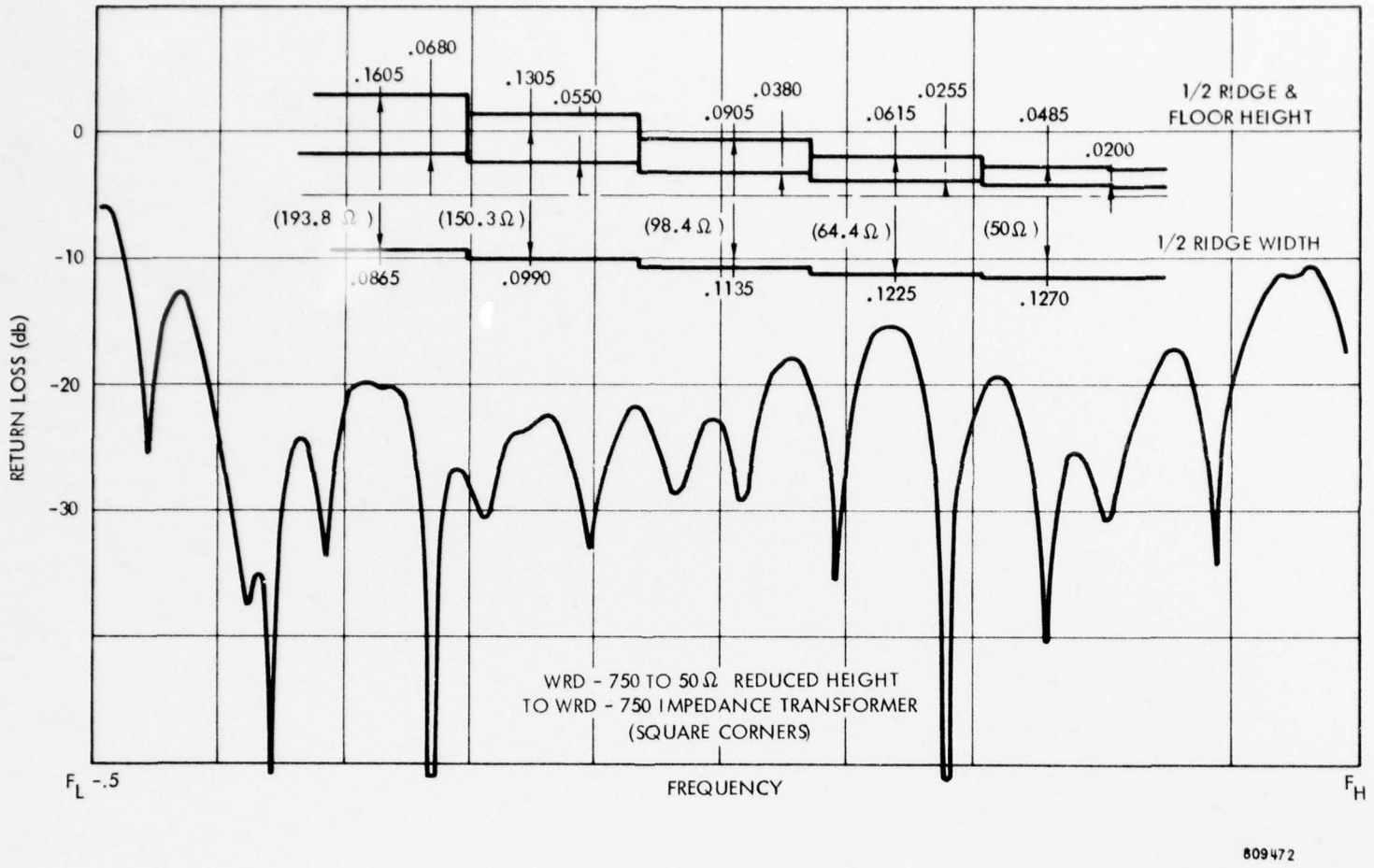

Figure 8-1. Waveguide Transistion Results

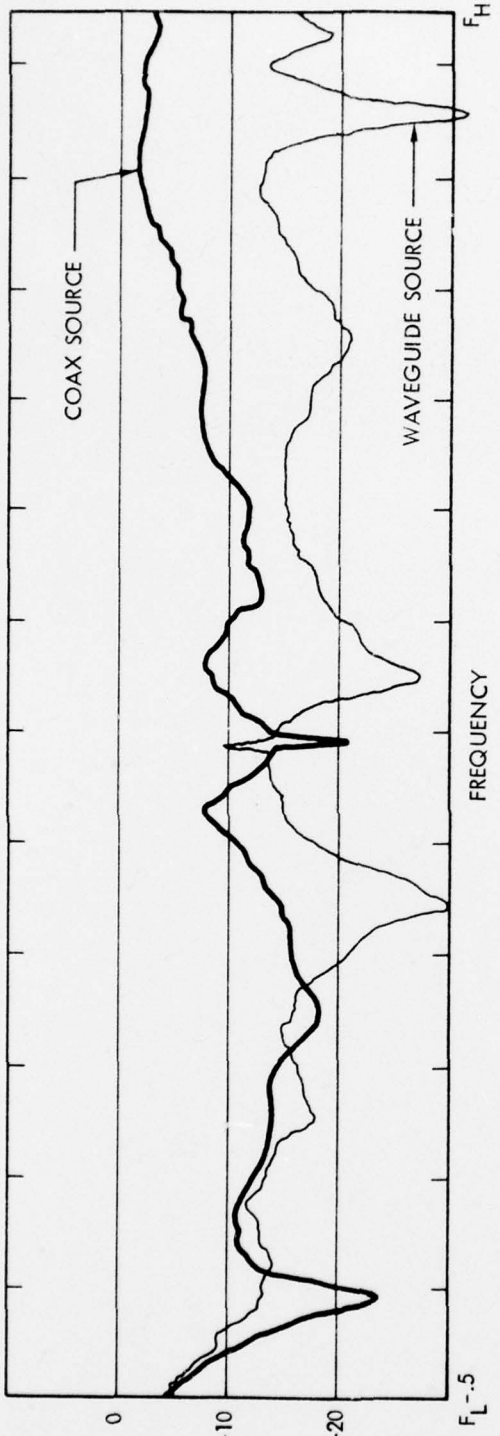

Figure 8-2. 50Ω Coax to Waveguide.

subassembly. They will, in turn, be loaded into a copper vacuum sleeve by heat shrinking. All ceramic edges are capable of 9400 volt minimum standoff at a gradient of 25 volts/-.001 inch. Thus, arcing, discharges and leakage problems should be minimal. The high voltage feedthroughs form a stacked up header similar to that used in electron guns but with external connections made at the header inner diameter. This approach eliminates vacuum pin seals (a common reliability problem) and provides an easily potted and shielded cavity for the high voltage lead terminations.

Various diameters have been considered for the collector. The collector design is dictated to some extent by packaging considerations. If more space is available in the system, the collector diameter can be increased, having a beneficial effect on the thermal densities in the conduction cooled package. Analysis of the package constraints has been started by Northrop to study the possible tube package configuration. Figure 9-1 shows a preliminary layout of the tube in the system boundaries. A thermal analysis has also been started by Northrop DSD. The results of this work are expected to provide sufficient input to the tube groups to allow a final collector design to be established. The rf bridge length of the final design will be established at the same time, since the collector - package area will determine the allowable bridge length.

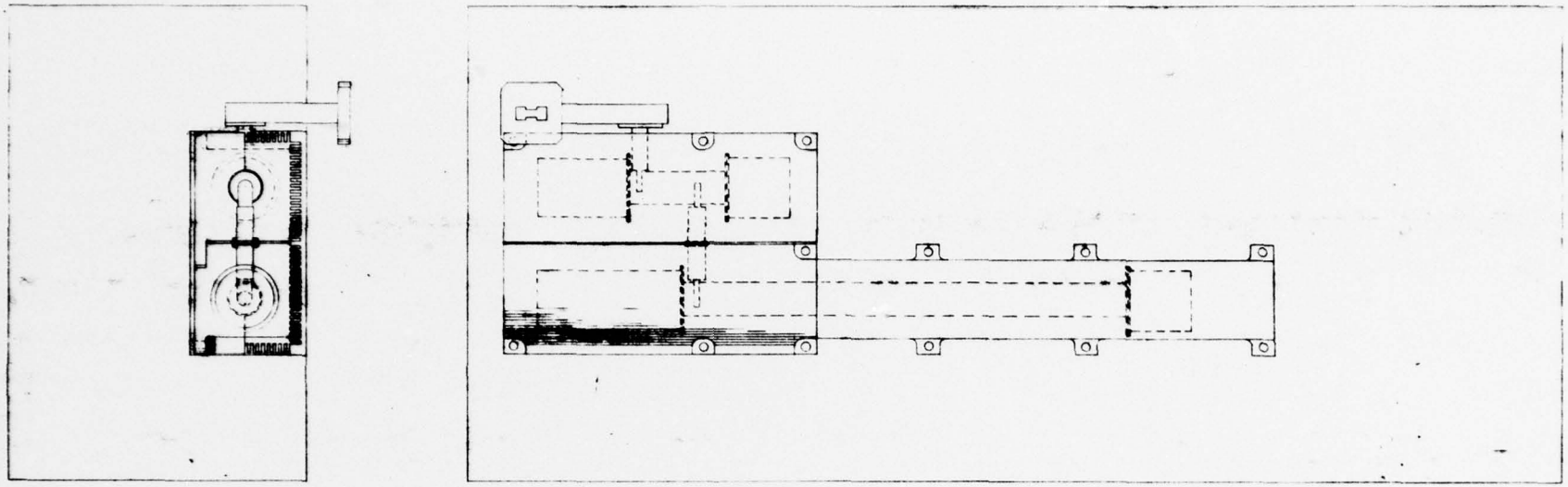

Figure 9-1. Preliminary Package Layout.

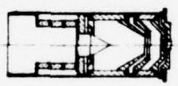

RAYTHEON 10-0231 (6/70)

PROJECT SCHEDULE

☐ IDP ☐ IRP

PROJECT TITLE	PROPOSAL NO.	PROJECT LEADER	DIVISION
Dual Mode - Combined Schedule 10/15/78		J. McCarthy	

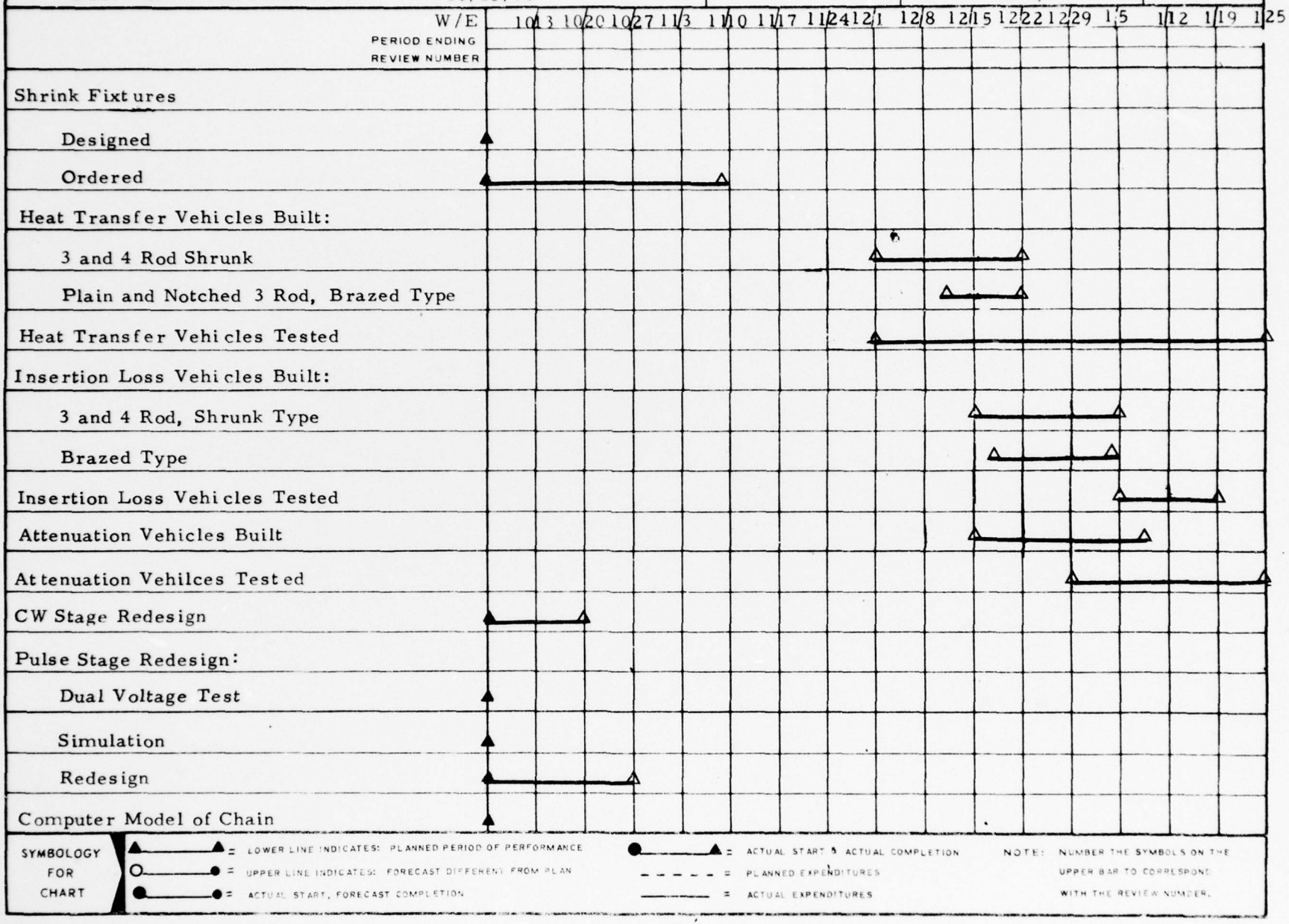

SYMBOLOGY FOR CHART

- = LOWER LINE INDICATES: PLANNED PERIOD OF PERFORMANCE
- = UPPER LINE INDICATES: FORECAST DIFFERENT FROM PLAN
- = ACTUAL START, FORECAST COMPLETION
- = ACTUAL START & ACTUAL COMPLETION
- = PLANNED EXPENDITURES
- = ACTUAL EXPENDITURES

NOTE: NUMBER THE SYMBOLS ON THE UPPER BAR TO CORRESPOND WITH THE REVIEW NUMBER.

RAYTHEON 10-0231 (6/70)

PROJECT SCHEDULE

☐ IDP ☐ IRP

PROJECT TITLE	PROPOSAL NO.	PROJECT LEADER	DIVISION
Dual Mode -Combined Schedule 10/15/78		J. McCarthy	

	W/E	10 13	10 20	10 27	11 3	11 10	11 17	11 24	12 1	12 8	12 15	12 22	12 29	1 5	1 12	1 19	1 25
	PERIOD ENDING																
	REVIEW NUMBER																
N	Evaluate Circuit and Bridge Match									△						△	
C	Develop Waveguide Transition	△														△	
N	Package Analysis in System	△	△														
C	Collector Design	△	△														
N	Procure Collector Parts	△													△		

SYMBOLOGY FOR CHART

- △——△ = LOWER LINE INDICATES: PLANNED PERIOD OF PERFORMANCE
- ○——● = UPPER LINE INDICATES: FORECAST DIFFERENT FROM PLAN
- ●——● = ACTUAL START, FORECAST COMPLETION
- ●——△ = ACTUAL START & ACTUAL COMPLETION
- – – – – = PLANNED EXPENDITURES
- ——— = ACTUAL EXPENDITURES

NOTE: NUMBER THE SYMBOLS ON THE UPPER BAR TO CORRESPOND WITH THE REVIEW NUMBER.

RAYTHEON 10-0231 (6/70)

PROJECT SCHEDULE

☐ IDP ☐ IRP

PROJECT TITLE	PROPOSAL NO.	PROJECT LEADER	DIVISION
Manpower Applied vs Plan - Raytheon Only Dual Mode 10/15/78		J. McCarthy	

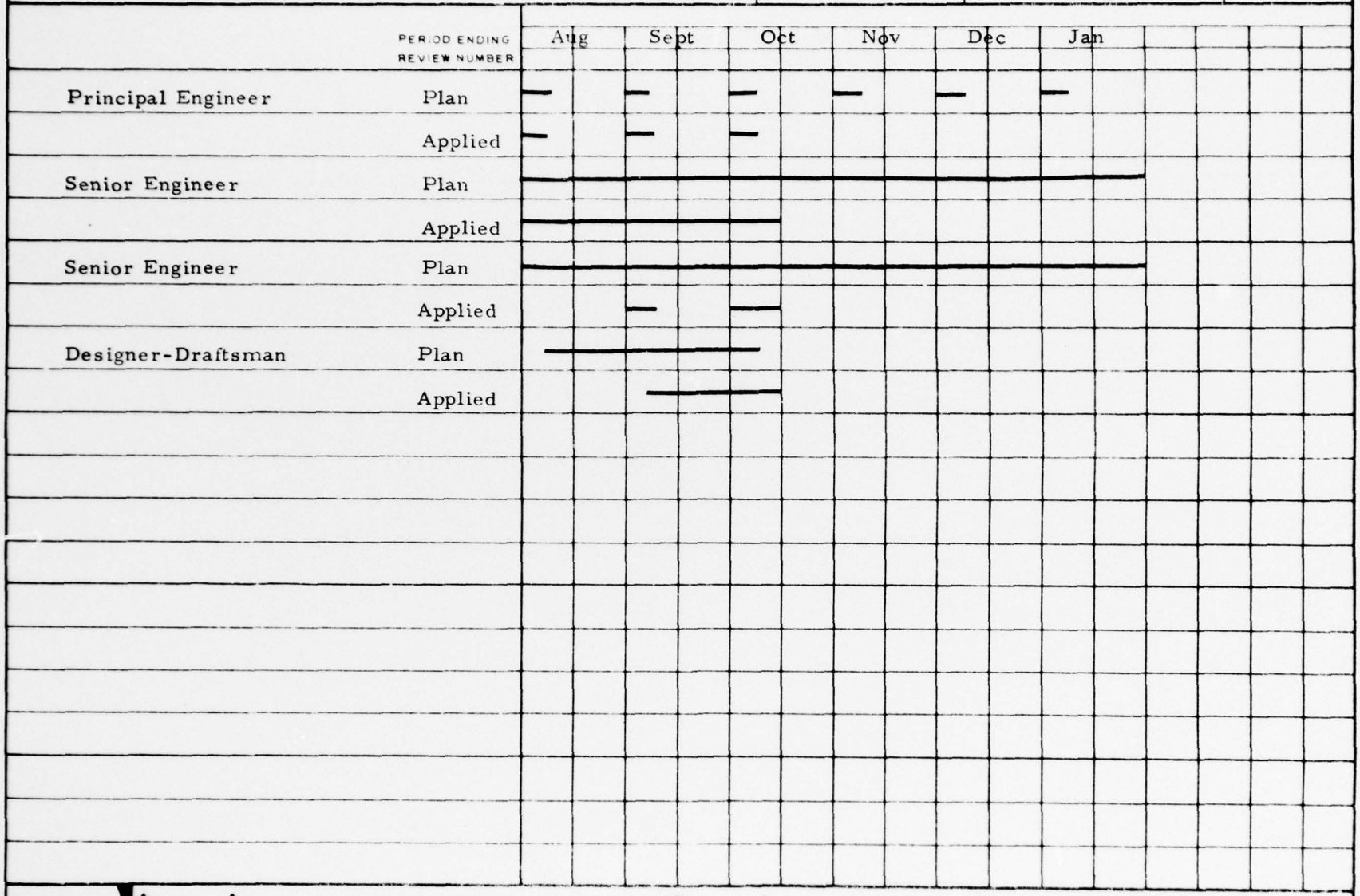

RAYTHEON 10-0231 (6/70)

PROJECT SCHEDULE

☐ IDP ☐ IRP

PROJECT TITLE	PROPOSAL NO.	PROJECT LEADER	DIVISION
Dual Mode Total Charges 10/15/78		J. McCarthy	P.T.